the plant journal

SEB SOCIETY FOR EXPERIMENTAL BIOLOGY

The Plant Journal (2020) **101,** 37–56 doi: 10.1111/tpj.14516

Cannabis glandular trichomes alter morphology and metabolite content during flower maturation

Samuel J. Livingston[1,†], Teagen D. Quilichini[1,2,†], Judith K. Booth[3], Darren C. J. Wong[4], Kim H. Rensing[5], Jessica Laflamme-Yonkman[1], Simone D. Castellarin[4], Joerg Bohlmann[1,3,4], Jonathan E. Page[1,2] and A. Lacey Samuels[1,*]

[1]*Department of Botany, University of British Columbia, Vancouver, British Columbia, Canada,*

[2]*Anandia Laboratories Inc., Vancouver, British Columbia, Canada,*

[3]*Michael Smith Laboratories, University of British Columbia, Vancouver, British Columbia, Canada,*

[4]*Wine Research Centre, University of British Columbia, Vancouver, British Columbia, Canada, and*

[5]*Fibics Inc., Ottawa, Ontario, Canada*

Received 2 April 2019; revised 28 July 2019; accepted 19 August 2019; published online 30 August 2019.

*For correspondence (e-mail lsamuels@mail.ubc.ca).

†Co-first authors, these authors contributed equally to this work.

SUMMARY

The cannabis leaf is iconic, but it is the flowers of cannabis that are consumed for the psychoactive and medicinal effects of their specialized metabolites. Cannabinoid metabolites, together with terpenes, are produced in glandular trichomes. Superficially, stalked and sessile trichomes in cannabis only differ in size and whether they have a stalk. The objectives of this study were: to define each trichome type using patterns of autofluorescence and secretory cell numbers, to test the hypothesis that stalked trichomes develop from sessile-like precursors, and to test whether metabolic specialization occurs in cannabis glandular trichomes. A two-photon microscopy technique using glandular trichome intrinsic autofluorescence was developed which demonstrated that stalked glandular trichomes possessed blue autofluorescence correlated with high cannabinoid levels. These stalked trichomes had 12–16 secretory disc cells and strongly monoterpene-dominant terpene profiles. In contrast, sessile trichomes on mature flowers and vegetative leaves possessed red-shifted autofluorescence, eight secretory disc cells and less monoterpene-dominant terpene profiles. Moreover, intrinsic autofluorescence patterns and disc cell numbers supported a developmental model where stalked trichomes develop from apparently sessile trichomes. Transcriptomes of isolated floral trichomes revealed strong expression of cannabinoid and terpene biosynthetic genes, as well as uncharacterized genes highly co-expressed with CBDA synthase. Identification and characterization of two previously unknown and highly expressed monoterpene synthases highlighted the metabolic specialization of stalked trichomes for monoterpene production. These unique properties and highly expressed genes of cannabis trichomes determine the medicinal, psychoactive and sensory properties of cannabis products.

Keywords: *Cannabis sativa*, glandular trichomes, fluorescence microscopy, electron microscopy, metabolite profiling, transcriptomics, cannabinoids, terpenes, DAPI.

INTRODUCTION

Cannabis sativa L. (cannabis) flowers are consumed for medicinal and recreational purposes based on the properties of their specialized metabolites (i.e. cannabinoids and terpenes). The metabolites are abundantly produced in the glandular trichomes on female flowers, which represent the valued 'marijuana bud', while male flowers are typically not consumed for recreational or medical purposes due to the scarcity of glandular trichomes. Cannabinoids synthesized in the glandular trichomes on female flowers include tetrahydrocannabinolic acid (THCA) and cannabidiolic acid (CBDA) (reviewed by Potter, 2009 and Pertwee, 2014). When heated, these molecules decarboxylate to their bioactive metabolites, tetrahydrocannabinol (THC) or cannabidiol (CBD), respectively. THC interacts with receptors in the human endocannabinoid system to produce psychoactive and therapeutic effects, while the non-intoxicating CBD has distinct pharmacological properties (Mechoulam, 1970; Pertwee, 2008). Cannabis terpenes include monoterpenes and sesquiterpenes, which are volatile and contribute to the fragrance of cannabis flowers and

cannabis products (Hillig, 2004; Fischedick *et al.*, 2010; Booth *et al.*, 2017; Booth and Bohlmann, 2019; Mudge *et al.*, 2019; Zager *et al.*, 2019). Terpenes have been proposed to act synergistically with cannabinoids to elicit the pharmacological effects of cannabis consumption (Russo, 2011). Despite the economic and medicinal importance of cannabis glandular trichomes, the properties and relative contributions of the different types of cannabis glandular trichomes remain poorly understood.

On female cannabis flowers, three types of glandular trichome have been described based upon their surface morphology: bulbous, sessile, and stalked (Hammond and Mahlberg, 1973). Bulbous trichomes are the smallest in size and produce limited specialized metabolites (Potter, 2009). Sessile trichomes of cannabis sit on the epidermis with a short stalk and have a globose head comprised of a multicellular disc of secretory cells and a subcuticular metabolite storage cavity (Hammond and Mahlberg, 1977). By comparison, stalked trichomes of cannabis have a similarly shaped, slightly larger, globose head elevated several hundreds of microns above the epidermal surface by a multicellular stalk (Mahlberg and Kim, 2004; Potter, 2009). The relative contributions of the two major glandular trichome types, sessile and stalked, to the cannabinoid and terpene profiles of cannabis flowers are unknown.

Anatomic and metabolic specialization of glandular trichomes has been demonstrated in other well characterized glandular trichome systems, including Lamiaceae and Solanaceae (Simmons and Gurr, 2005; Huang *et al.*, 2008; Schilmiller *et al.*, 2009). For these taxa, glandular trichomes are considered to fall into two categories: peltate trichomes, which are analogous to sessile as they sit on the organ surface, and capitate trichomes that have a long stalk above the epidermis (Glas *et al.*, 2012; Huchelmann *et al.*, 2017). The peltate type have eight secretory disc cells that produce an abundance of metabolites, often enriched in monoterpenes, which accumulate in a large subcuticular cavity, as detailed for peppermint (*Mentha* × *piperita*) (Turner *et al.*, 2000) and lavender (*Lavandula pinnata*) (Huang *et al.*, 2008). The second category, capitate glandular trichomes, have a large stalk holding a small head of one or few apical secretory cells and produce metabolites that are not stored in a subcuticular cavity (Glas *et al.*, 2012). Within the genus *Solanum,* different subtypes of capitate trichomes produce specific metabolites such as acyl sugars or terpenes (Schilmiller *et al.*, 2009; McDowell *et al.*, 2011). In cannabis, the stalked trichomes produce more total cannabinoids than sessile trichomes, which may be due to the relative differences in trichome head diameter (Turner *et al.*, 1978). The terpene profiles produced by individual trichome types have not been investigated. Whether specialization of metabolite production exists between cannabis stalked and sessile trichomes remains unknown.

Cannabis stalked trichomes resemble sessile/peltate trichomes superficially, but they are raised upon a large stalk (Potter, 2009). In both types, a disc of secretory cells develop a large extracellular storage cavity formed by delamination of the apical cell wall (Kim and Mahlberg, 1991, 2003). In fact, the morphological similarity between stalked and sessile gland heads has resulted in some reports classifying these two trichome types as a single group (Dayanandan and Kaufman, 1976). Additionally, a developmental relationship has been proposed, where sessile trichomes on flowers may represent a premature stage of stalked trichome development (Hammond and Mahlberg, 1977; Potter, 2009). It remains unclear if stalked trichomes are distinct from sessile trichomes simply by the presence or absence of a stalk, or whether stalked and sessile trichomes have additional unique characteristics.

The goal of this study was to proceed beyond the known surface features of cannabis glandular trichomes by characterizing their internal anatomy, biochemistry and transcriptome. The first objective was to define the metabolite storage cavity characteristics of cannabis stalked and sessile trichomes using *in vivo* intrinsic fluorescence. The second objective was to test the hypothesis that stalked trichomes on flowers develop from sessile-like precursors. Thirdly, we performed chemical and transcriptomic analysis of stalked trichomes, and sessile-like premature stalked trichomes, to determine whether metabolic specialization occurs in cannabis trichomes, and to explore the gene co-expression networks of CBDA synthase during cannabinoid biosynthesis and storage.

RESULTS

Stalked glandular trichomes have unique blue intrinsic fluorescence

In this work, we used 'Finola', a hemp variety known for its short stature and accelerated flowering time, making it economically important and useful for research purposes (van Bakel *et al.*, 2011; Sawler *et al.*, 2015). The female plants produced clusters of individual flowers (florets) surrounded by bracts (Figure 1a). Each floret consisted of two protruding styles attached to an ovule, which was enclosed by a calyx covered with metabolite-rich trichomes (Figure 1b,c). Calyces and bracts were covered with non-glandular hairs, as well as glandular trichomes. Trichome density was highest on calyces, therefore these were used for the characterization of glandular trichomes. Although different trichomes on the calyx are apparent with conventional scanning electron microscopy (SEM) (Figure 1c; Video S1), trichome morphology was sometimes damaged by sample preparation. Therefore, we used cryo-SEM to examine the trichomes in their native state, without fixation, to view the external morphology while retaining the metabolites of the storage cavity. The heads of stalked

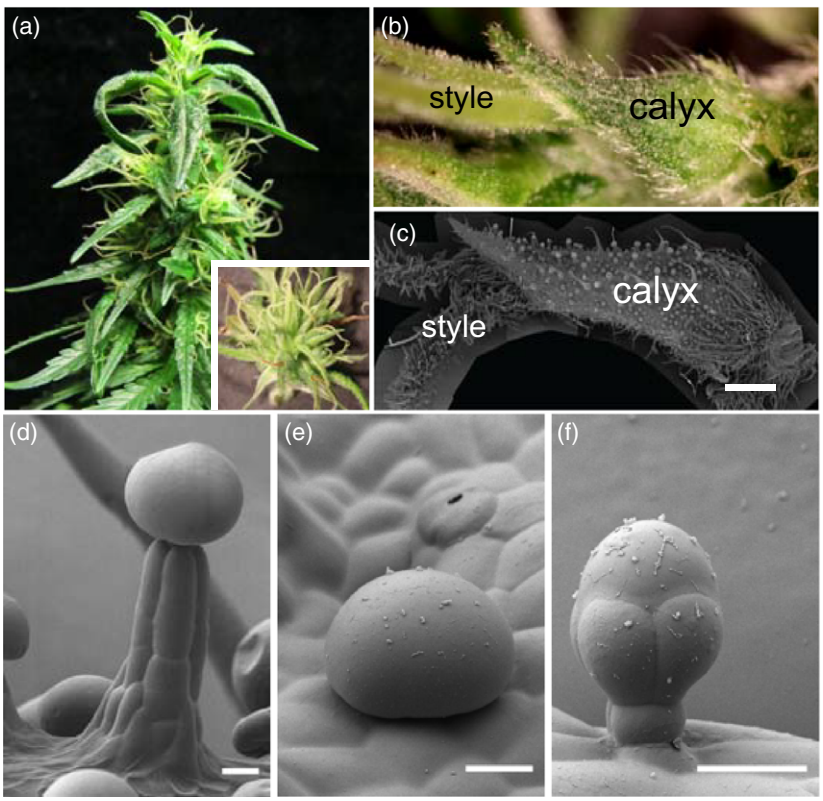

Figure 1. The three types of glandular trichomes on female cannabis flowers.
(a) Flowering female 'Finola' plant; inset: isolated floral cluster containing numerous calyces bearing densely populated glandular trichomes. (b) Dissecting microscope image of the calyx and styles of an individual female flower. (c) Image of the calyx of an individual female flower using conventional SEM; scale bar 500 μm. (d–f) Cryo-SEM images of the three types of cannabis glandular trichomes, classified as stalked (d), sessile (e), and bulbous (f); scale bars 20 μm.

glandular trichomes were elevated above the epidermis on a multicellular stalk (Figure 1d) and sessile trichomes sat directly on the epidermis (Figure 1e). Bulbous trichomes had diminutive size and a small storage cavity (Figure 1f).

To investigate how the trichomes accumulate lipidic metabolites in the storage cavity, the internal structures of each type of trichome were probed using multi-photon imaging. We developed a two-photon laser scanning fluorescence microscopy approach, where a red-shifted pulsed laser is used to penetrate deep into live tissues and excite the intrinsic fluorescence of metabolites. Spectral scans of trichome cavities revealed substantial emission intensity between 420–530 nm (Figure 2a). Two spectral emission windows were used for imaging: 420–460 nm, which was false-coloured teal; and 495–540 nm, which was false-coloured red (Figure 2a). Merging these spectral windows produced a high resolution three-dimensional data set of live cannabis trichomes, which revealed striking differences in fluorescence emission and the storage cavity internal morphology between stalked, sessile and bulbous trichomes of calyces. Within the extracellular storage cavity, stalked glandular trichomes contained one large droplet with blue-shifted fluorescence and some smaller droplets in the surrounding dark non-fluorescent matrix (Figure 2b). Sessile trichomes from calyces (Figure 2c) displayed numerous small droplets with red-shifted fluorescence within the cavity. Similar fluorescence and arrangements of metabolites were observed in sessile trichomes from leaves (Figure 2d) and anthers (Figure 2e). Bulbous trichomes observed on leaves and florets had blue-shifted cells and a very small red-shifted cavity (Figure 2f). The fluorescence emission and droplet arrangements observed in 'Finola' trichomes are consistent with trichomes of high-THCA medicinal varieties 'Purple Kush' and 'Hindu Kush' (Figure S1a–c). Pure cannabinoids fluoresce with a peak emission at 430 nm (Hazekamp *et al.*, 2005), which falls within the broad 460 nm peak observed from stalked glandular trichomes. The interpretation that the strong blue-shifted fluorescence of stalked trichomes reflects high cannabinoid content is supported by previous reports showing stalked trichomes have the highest cannabinoid storage of the three trichome types (Turner *et al.*, 1978; Mahlberg and Kim, 2004; Potter, 2009). To further examine the metabolite arrangements in storage cavities, transmission electron microscopy was performed, revealing many small droplets of metabolites within the cavity of sessile trichomes and a large central droplet within the cavity of stalked trichomes (Figure 2g,h). Combined, our microscopy approaches show that trichomes on mature cannabis organs can be distinguished not only by whether they sit on the epidermis or a stalk, but also by their intrinsic fluorescence and the arrangements of metabolites in their storage cavities. The strong blue autofluorescence of the stalked glandular trichomes,

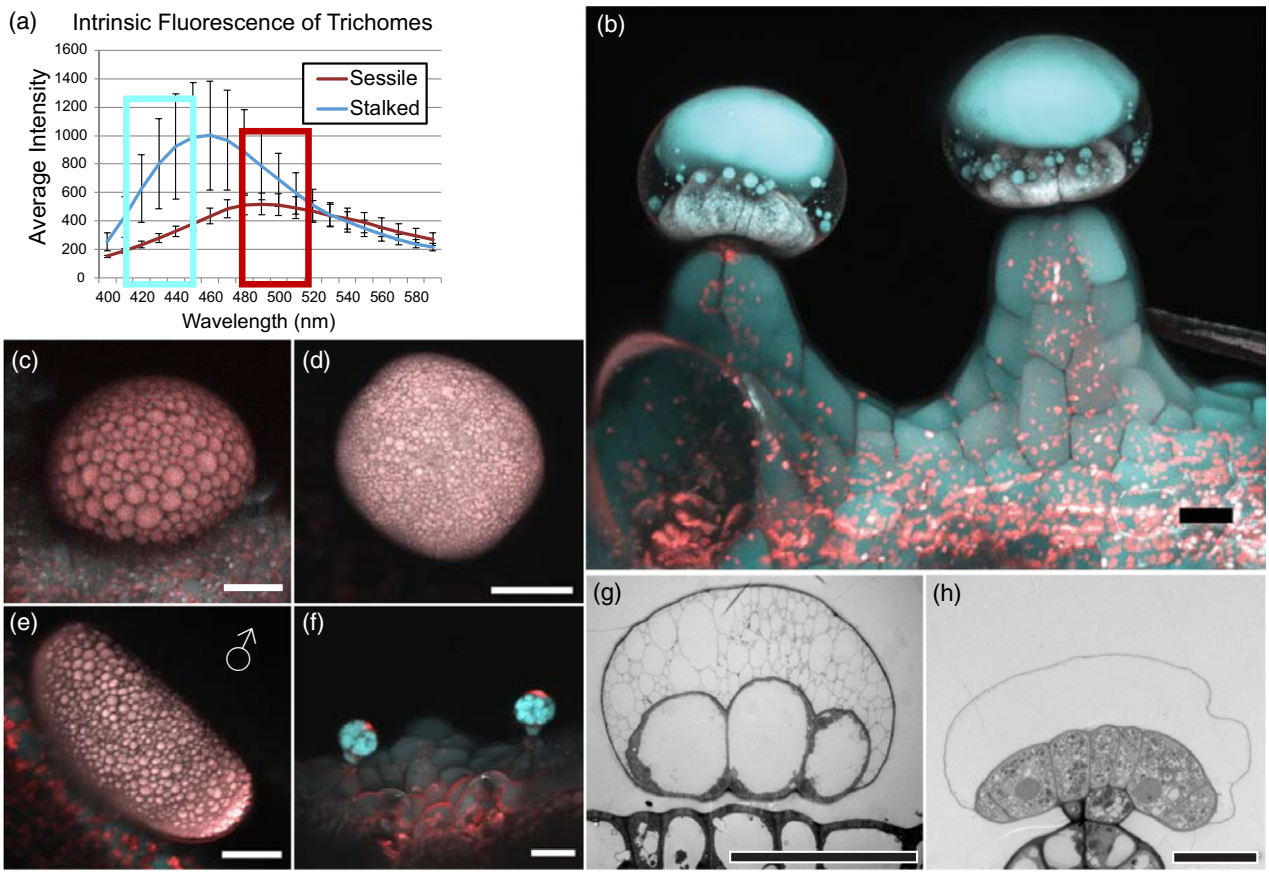

Figure 2. Glandular trichomes exhibit distinct intrinsic fluorescence and metabolite organizations.
(a) Plot of mean ± SD emission intensity against wavelength (nm) shows trend towards lower wavelength emissions from stalked trichome cavities. (b-f) Multi-photon microscopy images of the glandular trichomes on cannabis plants, including female calyx stalked (b), calyx sessile (c), leaf sessile (d), male antherial sessile (e), and calyx bulbous (f), revealing distinct organization and intrinsic fluorescence of the metabolites stored in the storage cavity. (g, h) Transmission electron micrographs of sessile glandular trichome (g) with many droplets in storage cavity, and a stalked glandular trichome (h) with large central droplet of metabolites in storage cavity. Scale bars 25 μm.

contrasted with red-shifted autofluorescence in sessile and bulbous trichomes, provide diagnostic characteristics for each trichome type.

Stalked glandular trichomes have many secretory disc cells

If stalked trichomes are simply sessile trichomes elevated on a multicellular stalk, then the arrangement and number of secretory disc cells forming the base of the globose head should be similar between stalked and sessile. Preliminary observations suggested that cannabis floral glandular trichomes had 'a flattened disc of few to many cells' (Hammond and Mahlberg, 1973). Subsequent reports indicated that sessile (Potter, 2009) and stalked trichomes (Dayanandan and Kaufman, 1976) have eight cells, or that stalked trichomes have eight to thirteen cells (Hammond and Mahlberg, 1977). However, the number of cells in different trichome types was difficult to resolve (Potter, 2009). To test the hypothesis that the different trichome types had different numbers of cells in their secretory disc, samples were fixed, cleared, and stained with DAPI to show nuclei (Figure 3). Sessile trichomes consistently had exactly eight cells on mature leaves (100%, $n = 21$; Figure 3a) and on mature calyces (78.6%, $n = 14$; Figure 3b). In contrast, the large stalked glandular trichomes on mature calyces had the largest and most variable number of cells, typically 12–16 cells (Figure 3c). Because the inconspicuous storage cavities of bulbous trichomes could not be distinguished from undifferentiated pre-secretory trichomes after fixation and clearing, only stalked and sessile trichomes with mature cavities were included in this analysis. Stalked trichomes on mature calyces had statistically significantly more cells in their secretory discs than the sessile trichomes of either mature calyces or vegetative leaves (Figure 3d). In addition, the trichome disc cell numbers of a high-THCA cannabis variety, 'Purple Kush', were quantified to test if the larger number of cells within stalked trichomes was also observed in 'drug-type' varieties. As with the hemp variety, sessile trichomes had exactly eight cells while stalked trichomes had the largest

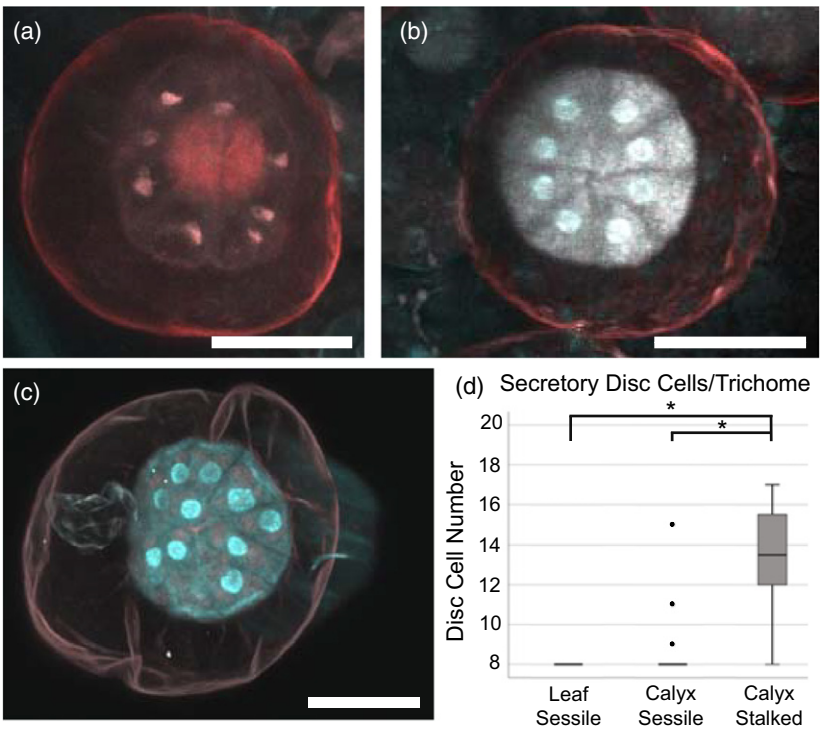

Figure 3. Stalked glandular trichomes on mature cannabis flowers have a proliferation of cells in their secretory disc.
(a–c) Multi-photon microscopy images of disc cell nuclear labelling for leaf sessile (a), calyx sessile (b) and calyx stalked (c) glandular trichomes; scale bars 25 μm. (d) Box plot showing disc cell number of leaf sessile ($n = 21$), calyx sessile ($n = 14$), and calyx stalked ($n = 22$) trichomes. Center line indicates median; box limits indicate 1st (lower) and 3rd (upper) quartiles; whiskers indicate minimum and maximum data points; black circles indicate outliers; $*P < 0.001$, non-parametric pair-wise comparisons using Dunn's procedure with a Bonferroni correction.

and most variable number of cells in the secretory disc (Figure S1d). These data indicated that cannabis sessile and stalked glandular trichomes are distinct, with stalked glandular trichomes having greater numbers of secretory disc cells.

Stalked glandular trichomes dominate the mature female flowers

To test the hypothesis that stalked trichomes may develop from sessile trichomes on cannabis florets, the distributions of stalked and sessile trichomes on the cannabis calyx were mapped during development. SEM with an image tiling and collection system (Atlas) was used to obtain maps of whole calyces that could be magnified to single trichome resolution (Video S1). Stalked trichomes were scarcely observed on short calyces (Figure 4a), whereas more mature, longer calyces possessed an abundance of stalked trichomes (Figure 4b). Quantification of trichomes using the Atlas system revealed a positive correlation between calyx length and the percentage of stalked trichomes present ($R^2 = 0.74$) (Figure 4c). Throughout the development of the calyx, the proportion of stalked trichomes increased from less than 30% to 80–90% for the most mature calyces. These data support the hypothesis that stalked trichomes develop from sessile glandular trichomes. In addition, the high proportion of stalked trichomes on mature florets indicates that the characteristics of the stalked trichomes will dominate the pharmacological and sensory properties of cannabis flowers.

Floral stalked trichomes develop from trichomes that appear sessile

The hypothesis that stalked trichomes develop from sessile trichomes was historically difficult to test using surface morphology alone. Time-lapse movies of intact calyces on dense floral clusters of intact plants, or isolated calyces in tissue culture, proved technically challenging to achieve within the constraints of regulatory permits. Therefore, we re-examined the trichomes of immature calyces using our diagnostic criteria for sessile and stalked trichomes, reasoning that if sessile trichomes were maturing into stalked trichomes, then the intrinsic fluorescence properties and droplet organization in the storage cavity should change from the red-shifted small droplets of sessile trichomes on calyces, vegetative leaves, and anthers (Figure 2c–e) to the blue-shifted large droplets seen in stalked trichomes (Figure 2b). The intrinsic fluorescence properties of trichome cavities were imaged with two-photon microscopy (Figure 4d). The largest droplet in the cavity and the ratio of total cavity fluorescence intensity in the 'teal channel' of 420–460 nm over the 'red channel' of 495–540 nm were measured for stalked and sessile trichomes (Figure 4e). A Kruskal–Wallis test was conducted to determine if there were differences in fluorescence ratio and droplet size between stalked trichomes from calyces, sessile trichomes from calyces and sessile trichomes from vegetative leaves. Fluorescence ratios and droplet size differed significantly between the three glandular trichome groups,

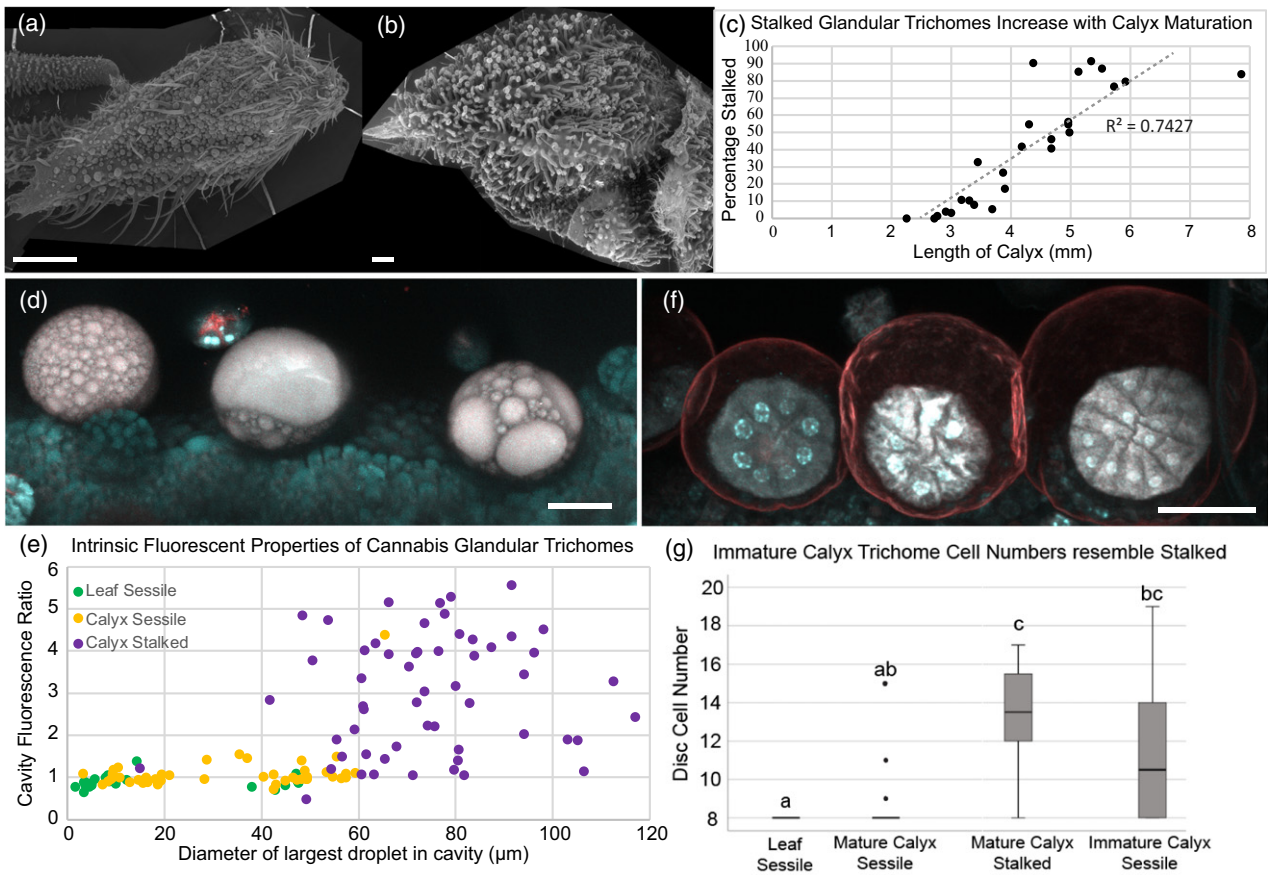

Figure 4. Sessile-like trichomes on calyces develop into stalked glandular trichomes.
(a, b) Atlas SEM images of an immature (a) and a mature (b) calyx; scale bars 0.5 mm. (c) Positive correlation of percentage of stalked trichomes and calyx length. (d) Multi-photon microscopy image of three sessile trichomes on a calyx; scale bar 50 µm. (e) Quantitative measurements of cavity fluorescence ratio (teal channel signal/red channel signal) of leaf sessile (n = 28), calyx sessile (n = 45), and calyx stalked glandular trichomes (n = 53). Dots represent individual trichome measurements. (f) Nuclear labelling with DAPI of sessile trichomes on an immature calyx; scale bar 50 µm. (g) Box plot revealing disc cell numbers in leaf sessile (n = 21), mature calyx sessile (n = 14), mature calyx stalked (n = 22), and immature calyx sessile (n = 32). Center line indicates median; box limits indicate 1st (lower) and 3rd (upper) quartiles; whiskers indicate minimum and maximum data points; black circles indicate outliers; letters above boxes indicate statistically significant groups (P < 0.001) determined by post-hoc non-parametric pair-wise comparisons using Dunn's procedure with a Bonferroni correction for multiple comparisons.

$\chi^2(2) = 80.588$, $P < 0.0005$ and $\chi^2(2) = 90.310$, $P < 0.0005$ respectively (Figure S2). Post-hoc pair-wise comparisons using Dunn's procedure with a Bonferroni correction for multiple comparisons revealed statistically significant differences in fluorescence ratio and droplet size among each set of the three trichome types (Figure S2). Plotting teal:red fluorescence ratio as a function of droplet size (Figure 4e) demonstrated that the sessile trichomes on the calyx displayed intermediate cavity droplet arrangements and fluorescence ratios between the sessile trichomes of a vegetative leaf and the stalked trichomes of a calyx. Therefore, the fluorescence properties of the metabolites are consistent with many of the apparently sessile trichomes on calyces representing premature stalked trichomes.

Examining the cell numbers in the secretory disc provided a second line of evidence in support of the hypothesis that a subpopulation of sessile trichomes on developing flowers are a premature developmental stage of stalked trichomes. If the sessile trichomes on an immature calyx are actually premature stalked trichomes, they are predicted to have greater than eight cells. If they are similar to sessile trichomes on vegetative leaves (which do not produce stalked trichomes), they are predicted to contain only eight cells. The majority of sessile trichomes on immature calyces had greater than eight cells (Figure 4f,g). Even pre-secretory trichomes on calyces that lacked a storage cavity were more likely to contain greater than eight cells (75%, n = 32) than to have only eight cells (25%, n = 32). These data indicate that the majority of premature trichomes sitting on the epidermal surface of developing calyces have cell numbers similar to stalked glandular trichomes on mature calyces.

Although most of the sessile trichomes on immature flowers appear destined to become stalked as the calyx matures, a scant subpopulation of sessile trichomes persisted. On mature calyces, the secretory disc cell numbers

of sessile trichomes with no stalk were more variable (79% had eight cells, and 21% had greater than eight cells; $n = 14$) than mature vegetative leaves (Figure 4g). A binomial logistic regression was performed to ascertain the effect of disc cell number on the likelihood of a trichome to have a stalk on mature leaves and calyces. The logistic regression model was statistically significant, and the model correctly classified 88% of cases ($\chi^2(1) = 33.687$, $P < 0.0005$). Based on our model, we could predict that 86% of secretory trichomes with more than eight cells are premature stalked trichomes, while 89% of secretory trichomes with eight cells are sessile trichomes, like those of vegetative leaves. Taken together, these data and the modeling indicate that stalked glandular trichomes develop from premature stalked trichomes with greater than eight cells.

Calyx glandular trichomes are rich in cannabinoids, with monoterpene-dominant terpene profiles

If the majority of floral sessile trichomes are in the process of becoming stalked, then the sessile trichomes on immature calyces are predicted to be biochemically more similar to stalked trichomes on mature calyces, and share fewer characteristics with sessile trichomes on other mature organs such as vegetative leaves and anthers. We tested this prediction by sampling the metabolites of stalked and sessile trichomes using two methods: whole-organ immersion in pentane (Figure 5a–d) and individual trichome sampling using a pulled glass microcapillary tube guided by ultraviolet (UV) light (Figure 5e–i). Whole-organ immersion of immature calyces (defined as no conspicuous stalked trichomes, <4 mm calyx length), and mature calyces (defined as >70% stalked trichomes, >4 mm calyx length) revealed a substantial increase in monoterpenes during calyx maturation (Figure 5a). The terpene profile of individual 'Finola' hemp plants was highly variable (Figures S3 and S4), as previously reported (Booth *et al.*, 2017). However, the proportion of monoterpenes to sesquiterpenes was consistently high in surface extracts from both immature and mature calyces, in contrast to the sesquiterpene-rich metabolic profile from vegetative leaves (Figures 5b and S3). Unlike the variation in monoterpene:sesquiterpene ratios, individual cannabinoid components were similar between vegetative leaves and flowers, although floral tissue contained more total cannabinoids than leaf (Figure 5c,d). These chemical analyses indicate that on the flower, the transitory population of sessile trichomes are biochemically similar to stalked glandular trichomes, supporting a developmental model that the majority of sessile trichomes are actually premature stalked trichomes. In addition, the different terpene profiles of flowers compared with vegetative leaves suggests specialization of terpene, but not cannabinoid, metabolism in different cannabis glandular trichomes.

To specifically test if floral stalked trichomes had distinct chemical profiles from sessile trichomes, the metabolite-rich contents of individual trichomes' storage cavities were sampled using a microcapillary probe. The characteristic blue intrinsic fluorescence of the stalked trichomes, excited by a hand-held ultraviolet light (Figure 5e,f), provided a useful diagnostic indicator to guide the microcapillary probe to one trichome and extract the storage cavity contents (Figure 5g). The cavity contents were pooled and analyzed with gas chromatography and liquid chromatography to profile the terpenes and cannabinoids, respectively. As with the whole calyces, terpene profiles in samples collected from stalked trichomes were dominated by monoterpenes (92%), with a monoterpene:sesquiterpene ratio over 12 (Figures 5h and S4). As previously noted (Turner *et al.*, 1978), sessile trichomes on the epidermis of mature calyces could not be sampled without cross-contaminating with stalked trichomes, so sessile trichomes' storage cavity contents were sampled from anthers and vegetative leaves. Consistent with the whole vegetative leaf results, the individual sessile trichomes from vegetative leaves sampled by microcapillary contained very low monoterpenes compared to sesquiterpenes (Figures 5h and S4). Sessile trichomes from anthers also had lower monoterpene:sesquiterpene ratios than the stalked trichomes (Figure 5h). Microcapillary sampling of stalked and sessile trichomes revealed similar cannabinoid profiles between the trichome types (Figure 5i), in agreement with the whole-organ cannabinoid profiles. These data indicated that mature calyces, and the stalked glandular trichomes that cover their surfaces, accumulate abundant cannabinoids and monoterpene-rich terpenes that are distinct from sessile trichomes of anthers or vegetative leaves that have lower monoterpene:sesquiterpene ratios. Therefore, the *bona fide* sessile trichomes found on anthers and vegetative leaves, which do not develop into stalked trichomes, have chemically distinct terpene profiles from the premature stalked and mature stalked glandular trichomes of cannabis flowers.

Isolated floral trichomes' transcriptome is enriched in cannabinoid and monoterpene biosynthetic genes

Transcriptomic studies from isolated trichomes have provided important insights into the gene expression underlying the specialized metabolism specifically within glandular trichomes (Lange, 2015a; Huchelmann *et al.*, 2017; Zager *et al.*, 2019). A previous study of the cannabis transcriptome examined various organs of cannabis including whole flowers at early, mid and late stages of flowering (van Bakel *et al.*, 2011); however, these floral transcriptome datasets included a mixture of glandular trichome types in addition to the underlying floret tissues. To explore potential differences in gene expression among the isolated floral trichome types, trichomes were

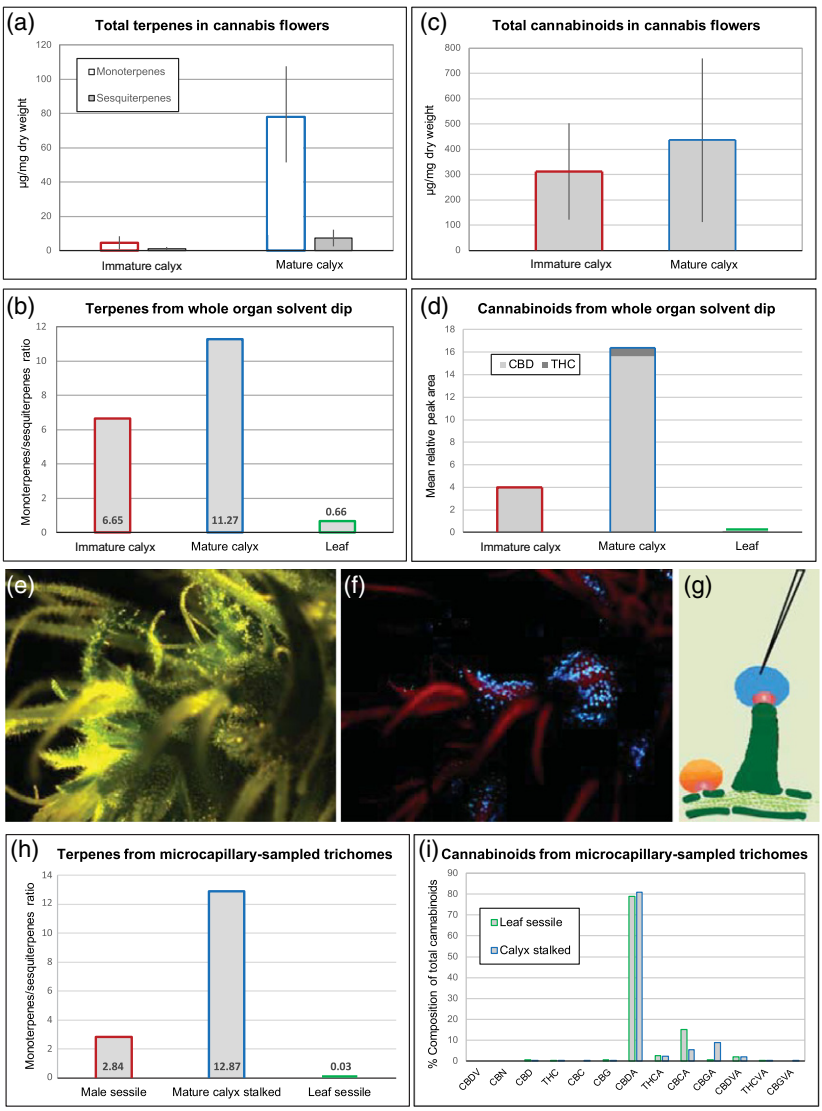

Figure 5. Mature calyces and microcapillary-sampled stalked glandular trichomes have monoterpene-dominant terpene profiles.
(a) Absolute levels of monoterpenes and sesquiterpenes from developing whole calyces dipped in solvent showing increases in monoterpenes as calyces mature. (b) The ratio of monoterpenes:sesquiterpenes is high in both immature calyces, with predominantly premature stalked trichomes, and mature calyces, with stalked trichomes. Leaves, which produce exclusively sessile trichomes, have more sesquiterpenes. (c) Absolute levels of cannabidiolic acid, mean ± SE, $n = 5$ plants with three technical replicates per plant. (d) Relative amounts of total cannabinoids in immature calyx and mature calyx compared to low levels in leaf; $n = 5$ plants with three technical replicates per plant. (e–g) A floral cluster (e), illuminated with ultraviolet light (f) to produce blue fluorescence from stalked glandular trichomes to assist microcapillary sampling of resin, as shown in (g). (h) The ratio of monoterpenes:sesquiterpenes from microcapillary sampling of storage cavities from anther sessile trichomes, floral stalked trichomes or leaf sessile trichomes. (i) The cannabinoid profiles of microcapillary-sampled storage cavities of floral stalked trichomes (100 cavities each) and leaf sessile trichomes (200 cavities each), $n = 3$ plants with three technical replicates per plant.

physically isolated from 'Finola' flowers, and enriched by type using a Percoll step centrifugation. Trichomes were separated from mid-stage flowers into three categories: the very small bulbous; pre-stalked trichomes with intermediate size and red-shifted fluorescence; and mature stalked with their larger size and blue-shifted intrinsic fluorescence. The pre-stalked category would include the minor subfraction of trichomes that would persist as sessile at maturity. RNA quality was assessed by gel electrophoresis and NanoDrop spectroscopy. Nine cDNA libraries encompassing three biological replicates for bulbous, pre-stalked trichomes and mature stalked were constructed and sequenced on an Illumina HiSeq 2500. In total, 98 million (M) paired-end reads (101 bp) were obtained after adaptor removal, trimming, and quality filtering with an average of 10 M paired-end reads/sample. The average number of surviving reads that were successfully mapped to both 'Finola' (FN) and 'Purple Kush' (PK) reference transcriptomes (van Bakel *et al.*, 2011; Data S1; Table S1) were 7.8 M.

As a first step to understand the important metabolic pathways within each trichome type, highly expressed genes were shortlisted and their functional annotation (i.e. MapMan BIN categories) assessed. Among the most highly expressed genes (ranked by descending fragment per kilobase of transcript per million (FPKM)) were those involved in mitochondrial electron transport, lipid metabolism, secondary metabolism (especially isoprenoids and terpenoids), glycolysis, citric acid cycle, and redox homeostasis in all trichome types (Data S1 and Figure S5). Interestingly, no statistically significant differences between stalked and pre-stalked trichomes were found (false discovery rate (FDR) > 0.05; Data S1). To determine which genes were differentially expressed in the floral

glandular trichomes during metabolite production, stalked (ST) and pre-stalked (PS) fractions were compared to isolated bulbous trichomes (BU), which were considered a less metabolically-productive epidermal outgrowth control. Analysis using MAPMAN annotated BIN categories showed higher enrichment for categories such as secondary metabolism, lipid metabolism, glycolysis and transport in ST-BU compared to PS-BU (Figures 6a and S6 and Data S2). Differential gene expression analysis revealed statistically significant differences (FDR < 0.05) between the glandular trichomes that produce high amounts of metabolites (ST or PS), and the less productive bulbous trichomes (Table S2 and Data S3).

Most genes involved in cannabinoid and monoterpene biosynthesis (Figure 6b) were detected in all trichome types (Figure 6c,d). The isolated trichomes expressed higher FPKM levels of the cannabinoid and terpene biosynthetic genes in glandular trichomes compared to the whole-organ transcriptomic data on mid-flower, root, and shoot from van Bakel *et al*. (2011) (Figure 6c,d). The isolated glandular trichomes had higher expression of the genes encoding enzymes of the two biochemical pathways leading to cannabinoid biosynthesis: geranyl diphosphate (GPP) production by the methylerythritol phosphate (MEP) pathway, as well as olivetolic acid production by extension and cyclization of hexanoate (Figure 6c,d). Our data support the proposed pathway for hexanoyl-CoA biosynthesis by the action of lipoxygenase (LOX), hydroperoxide lyase (HPL), and acyl-activating enzyme (AAE) (Stout *et al*., 2012) (Figure 6c,d; Table S3). The genes encoding enzymes that act on hexanoyl-CoA, tetraketide synthase (TKS, Taura *et al*., 2009; Gagné *et al*., 2012) and olivetolic acid cyclase (OAC, Gagné *et al*., 2012) were expressed at significantly higher levels in cannabis trichomes relative to all other genes (background) (Figure 6c,d and Data S3). Geranyl diphosphate synthase (GPPS), which occupies a central position in the biosynthesis of both cannabinoids and terpenes, was expressed at significantly higher levels in stalked and sessile glandular trichomes compared with bulbous (Figure 6c,d and Table S3). Genes encoding the final step of the cannabinoid pathway, which produce cannabigerolic acid (CBGA) by the combination of olivetolic acid and GPP by a prenyltransferase (PT), were highly expressed, as was cannabidiolic acid synthase (CBDAS) (Taura *et al*., 1996; Figure 6c,d and Table S2). Expression of transcripts for CBDAS and predicted upstream precursor pathways appeared to be coordinated, as many of the latter genes were strongly correlated (average Pearson's product-moment correlation coefficient [PCC] >0.8) with CBDAS expression (Figure 6e). This analysis revealed that the transcripts belonging to the proposed cannabinoid biosynthetic pathway are highly expressed in all floral glandular trichomes, with select transcripts highly expressed in stalked trichomes relative to bulbous trichomes. These findings are consistent with our chemical data, which do not support cannabinoid profile specialization amongst stalked and sessile trichomes (Figure 5).

As gene expression of plant specialized metabolic pathways often show signatures of co-regulation (Schilmiller *et al*., 2012; Lange *et al*., 2015b; Celedon *et al*., 2016), we performed gene co-expression analysis to prioritize novel candidate genes potentially relevant to cannabinoid and terpene metabolism as well as metabolite export and storage in the trichome. Our transcriptome compendium for co-expression consisted of the isolated trichome dataset, as well as the root, shoot, stem, and flowers (pre-, early- and mid/mature-flower) datasets of van Bakel *et al*. (2011). Using CBDA synthase as a query 'guide' gene, the top 300 co-expressed gene partners were retrieved (ranked by descending PCC values) (Data S4). These included candidate genes for enzymes of the hexanoate pathway that are currently uncharacterized, such as fatty acid omega-6 desaturase (FAD). Some of the most highly co-expressed genes are ATP-binding cassette (ABC) transporters of the ABCG subfamily, which have been demonstrated to export lipids in a variety of plant systems (Hwang *et al*., 2016). In addition, a suite of genes encoding cell wall-modifying enzymes was co-expressed with CBDAS, which may play a role in the expansion of the storage cavity cell wall to accommodate metabolite accumulation and storage. The co-expression relationships of CBDAS and selected highly co-expressed genes were plotted for root, shoot, stem, flower and isolated trichome data sets (Figure 7a). The co-expressed genes were highly specific to glandular trichomes and often showed little to no expression in vegetative tissues (Figure 7a). These analyses identify co-expressed genes with the cannabinoid pathway, expanding our knowledge of co-expressed genes related to metabolite export and cell wall expansion of cannabis floral trichomes.

Three of the genes that were most highly co-expressed with CBDAS (PCC ≥ 0.99) encode terpene synthases (TPS). These were cross-referenced with known TPS genes from 'Finola' (Booth *et al*., 2017) and other cannabis strains (Zager *et al*., 2019). The most highly co-expressed transcripts mapped to TPS3 (Table S4), a myrcene synthase (Booth *et al*., 2017). The product of this enzyme, myrcene, was a highly abundant monoterpene detected with gas chromatography (GC) in this study (Figures S3 and S4). The next two most highly co-expressed candidate terpene synthases (Figure 7a), CsTPS37FN and CsTPS38FN (named following Zager *et al*., 2019), were not previously characterized. Phylogenetic analysis placed these enzymes under the TPS-b clade of terpene synthases, suggesting they are monoterpene synthase enzymes (Figure S7). To exploit the transcriptome data and test the *in vitro* function of these putative TPS, CsTPS37FN and CsTPS38FN were produced by heterologous expression in *E. coli*, and their activity was tested with GPP as substrate. For CsTPS37FN, the

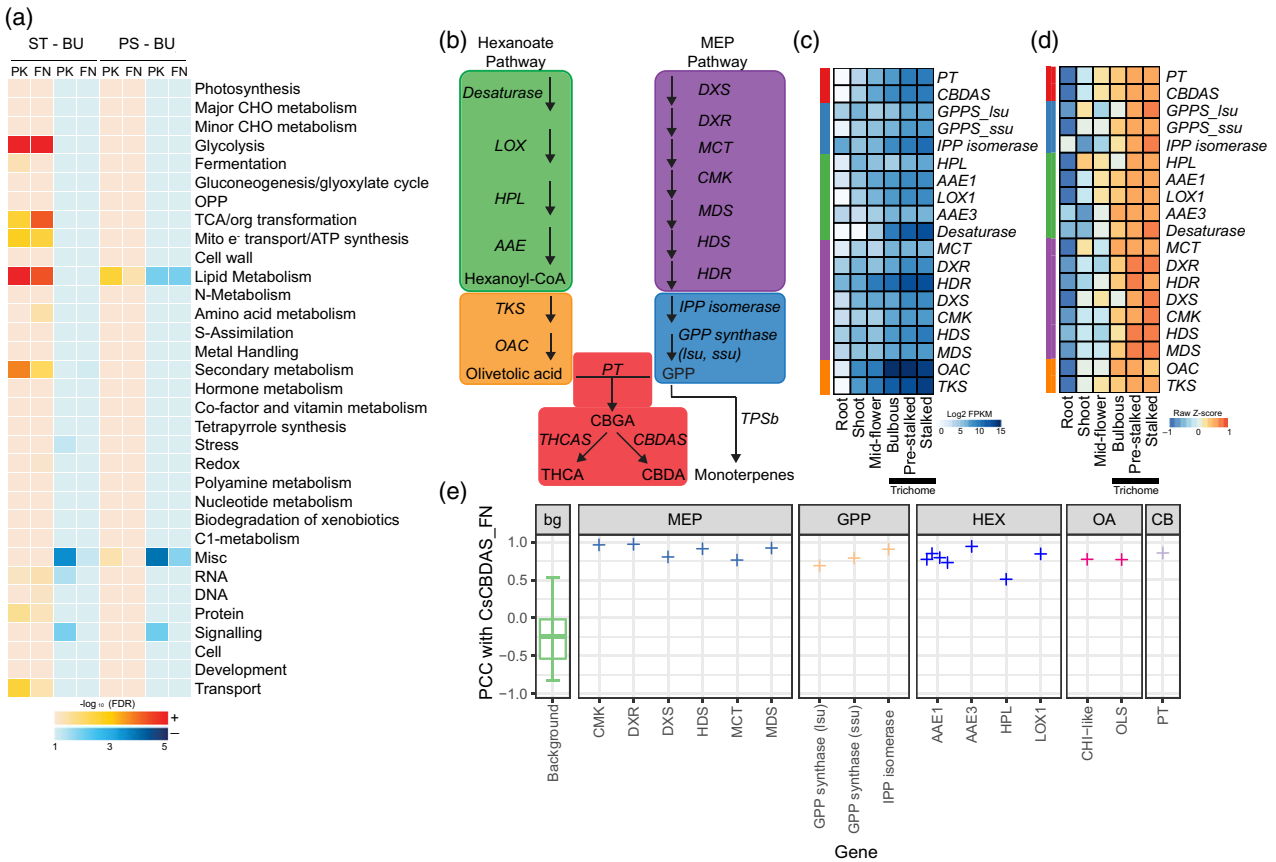

Figure 6. Transcriptomic analyses shows strong commitment to specialized metabolism by isolated cannabis trichomes.
(a) Enriched MapMan BIN functional categories of stalked (ST) versus bulbous (BU) and pre-stalked (PS) versus BU trichomes. Red/orange and blue colour depicts scores (expressed as −log10 FDR) of enriched categories for significantly upregulated and downregulated genes in each comparison. Both 'Purple Kush' (PK) and 'Finola' (FN) transcriptome annotations were used to complement each other's enrichment results. (b) Genes of the cannabinoid biosynthetic pathway from production of hexanoyl-CoA (green), olivetolic acid (orange), MEP pathway (purple), geranyldiphosphate (GPP- blue) and cannabinoids (red). Expression of selected genes in (b), presented as Log2FPKM (c) and raw Z-score (d) to highlight strong expression and enrichment in isolated trichomes, respectively. The whole-organ data of van Bakel *et al.* (2011) are shown for context, as specialized metabolite-related transcripts are enriched in isolated trichomes. (e) Pearson's product-moment correlation coefficient (PCC) of known genes involved in cannabinoid biosynthesis with CBDAS. Comparison of the observed PCC against all other genes (bg, background) shows strong transcriptional correlation of cannabinoid pathway biosynthetic genes with CBDAS.

dominant product was terpinolene, while recombinant CsTPS38FN produced (E)-β-ocimene (Figure 7b). Therefore, the co-expression analysis with CBDAS revealed previously uncharacterized monoterpene synthases, and their activity in producing terpinolene or (E)-β-ocimene is consistent with the monoterpenes detected by GC-MS (Figures S3 and S4). There was good agreement between the monoterpene-rich terpene profiles of floral stalked trichomes identified in our chemical analyses and the highly expressed monoterpene synthase genes (Table S4). These data provide another line of evidence that the stalked glandular trichomes have specialized to produce not only large amounts of cannabinoids but monoterpene-rich terpene profiles as well.

Overall, the transcriptomic analysis demonstrates that the glandular trichomes on cannabis flowers are strongly dedicated to cannabinoid and terpene production. The similarities between the mature stalked and floral premature stalked trichomes' transcriptomes provide an additional line of evidence supporting the model that the majority of calyx sessile trichomes develop into stalked trichomes as the flowers mature.

DISCUSSION

Glandular trichomes represent 'natural cell factories' (Huchelmann *et al.*, 2017), producing large quantities of specialized metabolites. In cannabis, the anatomic and metabolic distinctions between glandular trichome types on different plant organs were unclear. The findings presented here reveal that the sessile and stalked trichomes of cannabis differ not only in whether they sit on a large stalk or directly on the epidermal surface, they also have distinct fluorescent properties, number of cells in their secretory disc, and terpene metabolite profiles (Figure 8). The

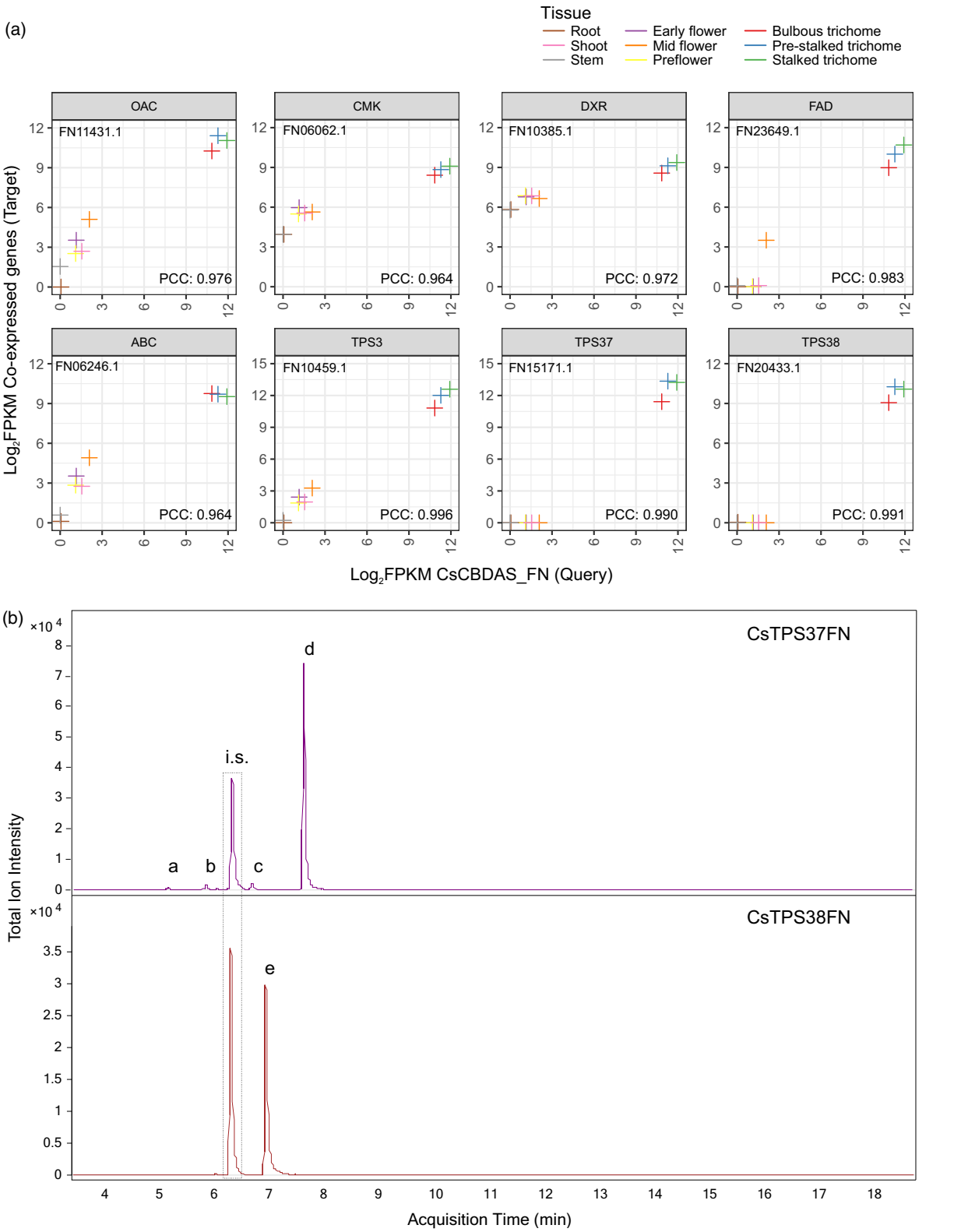

Figure 7. Co-expression analysis using CBDAS as a query reveals numerous genes putatively involved in metabolite biosynthesis, transport and storage.
(a) Co-expression relationship of CBDAS with selected highly co-expressed genes in various tissues and organs. The Pearson's product-moment correlation coefficient (PCC) depicts the co-expression strength of each interaction. (b) Products of CsTPS37FN (top panel) and CsTPS38FN (bottom panel) when incubated with GPP. a: α-pinene, b: β−pinene, c: limonene, d: terpinolene, e: (E)-β-ocimene. i.s., internal standard, isobutylbenzene.

stalked glandular trichomes of mature flowers have a globular head consisting of an enlarged disc of greater than eight secretory cells, which produce blue-shifted autofluorescent secretions rich in cannabinoids and monoterpenes. Conversely, sessile trichomes found on vegetative leaves have exactly eight secretory cells, produce red-shifted autofluorescent secretions with less cannabinoids and higher proportions of sesquiterpenes. We also show that stalked glandular trichomes are a terminal stage of development arising from sessile-like glandular trichomes on cannabis floral tissues. Trichome-specific transcriptomes generated here support this developmental model.

Investigations into glandular trichome structure and development using intrinsic fluorescence microscopy are still in their infancy. Recent studies have found that the glandular trichomes of some species, including tomato (Bergau *et al.*, 2015, 2016), Japanese catnip (Liu *et al.*, 2018), and lavender (Huang *et al.*, 2008) exhibit autofluorescent secretory cells and/or metabolites stored within their trichome cavities. A report using isolated snap-frozen stalked glandular trichomes of cannabis revealed autofluorescence in the secretory disc cells and their stalks, but not within the storage cavity (Ebersbach *et al.*, 2018). In contrast to these authors' findings, which used a longer excitation wavelength, our two-photon *in vivo* imaging of intact cannabis glandular trichomes revealed striking patterns of autofluorescence within the storage cavities of both stalked and sessile types on flowers and leaves. Of particular interest is the observation that a highly compartmentalized cavity was found in sessile trichomes of cannabis leaves and flowers, but not the stalked trichomes that dominate the mature flowers. Our data contrasts with previous reports using TEM that suggested a 'vesiculated' compartment is present in all cannabis trichome types (Mahlberg and Kim, 2004). In light of the data that supports stalked trichome development from sessile precursors on flowers, we hypothesize that co-incidental accumulation of monoterpenes and cannabinoids during stalk development remodels the apoplastic storage cavity from a highly compartmentalized state to fewer, larger droplets at maturity. The autofluorescence and two-photon microscopy revealed the *in vivo* metabolite storage patterns of cannabis glandular trichomes. Given the successful fluorescence activated cell sorting of tomato type VI glandular trichomes (Bergau *et al.*, 2016), the cannabis trichomes' autofluorescence observed here also may serve as a potential diagnostic feature for future studies.

In cannabis, both sessile and stalked glandular trichomes secrete and store varying proportions of monoterpenes and sesquiterpenes, in addition to the terpenophenolic cannabinoids. The cannabis 'sessile' glandular trichome is morphologically like the canonical peltate glandular trichomes (reviewed previously by Werker, 2000; Schilmiller *et al.*, 2008; Glas *et al.*, 2012; Tissier, 2012; Huchelmann *et al.*, 2017). These trichomes are well-characterized in the Lamiaceae family, the members of which produce economically important monoterpene-rich essential oils including peppermint, lavender and basil. Interestingly, our data demonstrate that the sessile trichomes of cannabis leaves, while they contain both monoterpenes and sesquiterpenes, do not follow the monoterpene-dominant pattern of other peltate-type trichomes.

The monoterpene-rich cannabis stalked glandular trichomes have gland heads similar in structure to sessile- or peltate-type trichomes, however, they sit on top of a multicellular stalk. Cannabis stalked glandular trichomes can be

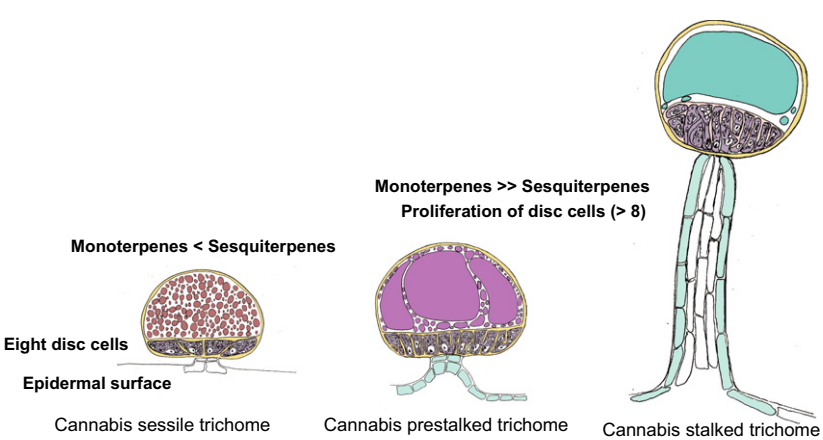

Figure 8. Unique features of stalked, pre-stalked and sessile glandular trichomes of cannabis. *Bona fide* sessile glandular trichomes (left) contain numerous small droplets of red-shifted intrinsic fluorescence, eight disc cells and sit directly on the epidermal surface. The sessile trichomes produce greater amounts of sesquiterpenes relative to monoterpenes. Stalked glandular trichomes (far right) develop from pre-stalked trichomes (center). Both pre-stalked and stalked trichomes have a greater number of disc cells, and they produce greater amounts of monoterpenes relative to sesquiterpenes. As the multicellular stalk lifts the glandular trichome head above the epidermis, the extracellular storage cavity is filled with a large droplet of blue-shifted intrinsic fluorescence, which is correlated with high cannabinoid content. Yellow indicates cuticle and cell wall surrounding the disc cells and storage cavity.

contrasted with capitate-type glandular trichomes of both the *Lamiaceae* and the *Solanaceae*, which have an elongated stalk that subtends only one or few secretory cells, and their specialized metabolites are often secreted onto the epidermal surface by pores formed in the cuticle (Tissier, 2012; Huchelmann *et al.*, 2017). Capitate-type VI tomato glandular trichomes secrete acyl sugars and terpenes into a small intercellular cavity between four secretory cells (Bergau *et al.*, 2015). Therefore, with respect to the proliferated secretory cells on top of the stalk and their ability to store large amounts of volatile compounds in a subcuticular cavity, the cannabis stalked glandular trichomes are atypical of capitate glandular trichomes in other species.

Our quantitative analysis and modeling show that stalked glandular trichomes arise from sessile-like premature stalked glandular trichomes on floral tissues, and this relationship may be predicted by the number of secretory disc cells upon cavity formation. These findings reveal that cannabis stalked glandular trichomes represent a terminal state of differentiation for floral sessile glandular trichomes, as opposed to the drastically different morphology and developmental trajectories of capitate and peltate glandular trichomes in other species. The similar results obtained from two-photon imaging and analysis of disc cell numbers among the hemp-type and medicinal-type varieties of cannabis confirm the relevance of our observations in diverse cannabis varieties. Recently, it was shown that cannabis varieties grown for medical consumption have larger gland heads on flowers when compared to cannabis strains grown for industrial fiber production (Small and Naraine, 2016), indicating selective pressure for larger glandular trichomes capable of producing greater amounts of cannabinoids and other secretory products. The larger heads in medicinal-type varieties may be the outcome of greater disc cell numbers in the gland head.

Previous studies of cannabis specialized metabolites have characterized the cannabinoid and terpene profiles of many cannabis strains, though the trichome-specific contributions to the overall plant's chemotype were not resolved. Stalked glandular trichomes are abundant on mature flowers (Turner *et al.*, 1977; Potter, 2009; Small and Naraine, 2016), and they store cannabinoids in higher abundance than sessile trichomes (Turner *et al.*, 1978). A study using laser capture microdissection sampling of different floral trichomes has been performed (Happyana *et al.*, 2013), however, non-glandular hairs were incorrectly classified as 'capitate-sessile trichomes', and therefore did not compare the sessile glandular trichomes as defined by others (Hammond and Mahlberg, 1973; Potter, 2009) to stalked trichomes. In our own microcapillary sampling, sessile and stalked trichomes were both dominated by CBDA, as expected for a hemp cannabis variety, with marginal variations in other cannabinoids. The cannabinoid quality was not different across cannabis trichome types and development, but the quantity clearly increased in floral stalked glandular trichomes.

In contrast with the cannabinoids, specialization of terpenes was found in our microcapillary sampling, with monoterpenes detected in higher proportions in floral stalked trichomes compared to vegetative and male sessile trichomes. Microcapillary sampling of individual sessile trichomes was previously performed (Malingré *et al.*, 1975), however the authors did not report terpene identity or compare with stalked trichomes. Most cannabis plants sampled have different amounts of the set of terpene compounds detected in this study (i.e. myrcene, α-pinene, (*E*)-β-ocimene, terpinolene, limonene, β-caryophyllene, and α-humulene) (Mediavilla and Setinemann, 1997; Meier and Mediavilla, 1998; Hillig, 2004; Potter, 2009; Aizpurua-Olaizola *et al.*, 2016; Booth *et al.*, 2017). Our sampling of fresh material resulted in a higher monoterpene to sesquiterpene ratio than was previously reported in samples that were dried for hours, weeks, or months (Ross and ElSohly, 1996; Hillig, 2004; Aizpurua-Olaizola *et al.*, 2016). Using fresh material, in which the more volatile monoterpenes are largely retained, gives a more accurate picture of the compounds produced in the glandular trichomes of cannabis plants. The monoterpene-rich stalked glandular trichomes dominate the mature cannabis flower, so understanding the molecular basis of variations in monoterpene profiles of this trichome type is important for understanding their impact on the sensory properties of cannabis products.

The transcriptomic and chemical analyses presented here show that the five most highly expressed terpene synthases from stalked glandular trichomes have monoterpene synthase activities that are consistent with the monoterpenes detected by microcapillary sampling of individual stalked trichomes and the whole calyx extracts. In a previous study of monoterpene synthases from 'Finola' (Booth *et al.*, 2017), the terpene synthase capable of producing terpinolene was not detected. In this study, the most highly expressed terpene synthase in the transcriptomes of the isolated glandular trichomes was characterized as the missing terpinolene synthase, completing the set of terpene synthases accounting for the major monoterpenes in the model cannabis strain 'Finola'.

The most highly expressed genes in isolated cannabis trichomes demonstrated not only a strong commitment to cannabinoid and terpene biosynthesis, but also high expression of genes related to primary metabolism, such as glycolysis, TCA cycle, and ATP synthesis (Figure 6). As demonstrated in a multi-omics study of tomato glandular trichomes, differentially expressed genes for these pathways are consistent with the high demands of metabolic productivity in glandular trichomes (Balcke *et al.*, 2017). While transcript abundance alone is insufficient to

quantitatively determine flux of central carbon metabolites through metabolic pathways (Xie *et al.*, 2008; Schwender *et al.*, 2014), the highly expressed central carbon and specialized metabolism BIN categories observed in cannabis glandular trichomes, in addition to the abundance of specialized metabolites stored by these structures, indicate a need for an abundance of carbon precursors and reducing power. The absolute flux, identity, and source of carbon precursors required for metabolite production in cannabis will require the types of detailed metabolomic analyses and flux modeling that have been done in tomato (Balcke *et al.*, 2017) and peppermint (Johnson *et al.*, 2017) glandular trichomes.

This study moves our knowledge of the properties of cannabis trichomes into the molecular age from the limited understanding based on the pioneering descriptive work of the trichomes' exteriors (Hammond and Mahlberg, 1973, 1977; Potter, 2009). Our findings support the hypothesis that the stalked glandular trichomes that densely cover the economically important cannabis flowers develop from transitory sessile-like precursors during floral development, and are anatomically and biochemically distinct from sessile trichome types on anthers and vegetative leaves. The spectroscopic and morphological features of 'Finola' glandular trichomes were also observed in medicinal high-THCA cannabis varieties, suggesting the conclusions drawn from the hemp-type 'Finola' variety may also be applied to other varieties of cannabis. Uncovering the unique properties of these economically and biotechnologically important structures, and the genes that are highly expressed within them, provides new opportunities for molecular breeding, targeted engineering, informed harvest timing and optimized processing of this important plant.

EXPERIMENTAL PROCEDURES

Plant growth

Female pistillate *Cannabis sativa* L. plants of the auto-flowering hemp-type variety 'Finola' were soil-grown from seed at Anandia Laboratories in Vancouver, British Columbia, in a Health Canada-permitted research laboratory. Seeds were planted into a soil mixture containing 1.5 tablespoons of Florikote™ (15-5-15) per 1 L scoop of soil (Sungro, Sunshine Mix #4). Plants were grown under T5 linear fluorescent lamps (Plusrite, FL54T5/865/HO), using an 18 h/6 h cycle (hours of light/hours of dark). Plants were watered with tap water for the first 2 weeks after planting and subsequently watered with Peter's Excel® (15-5-15) at a concentration of 0.05 tbsp L^{-1} (tablespoons per litre) for the duration of vegetative growth. Sterile bamboo stakes were used to support plant weight to best maintain an upright position when necessary. Biological controls were applied to the plants on a weekly basis. Female *Cannabis sativa* L. plants of the marijuana-type varieties 'Purple Kush' and 'Hindu Kush' were grown via clonal propagation. Clones were rooted in rockwool, then transferred directly into soil in a growth chamber (BC Northern Lights) under LED lights (BC Northern lights, 3000K 80 CRI spectrum). The plants were subjected to vegetative growth for 2–3 weeks using an 18 h/6 h light cycle and watered with Peter's Excel® (15-5-15). To induce flower development, the light cycle was switched to 12/12, and plants were watered with Maxibloom (5-15-14).

Two-photon microscopy

Fresh plant material was harvested from flowering 'Finola', 'Purple Kush' and 'Hindu Kush', and with the use of an Olympus SZX10 stereomicroscope, was dissected into vegetative leaves (1 mm^2 squares) and flowers (whole immature calyces- <4 mm length, no observable stalked trichomes; whole mature calyces- >4 mm length, >70% stalked trichomes). Dissected samples were affixed to double-sided scotch tape on a 25 × 75 mm microscope slide (Fisher) and mounted in distilled water prior to imaging on an Olympus Multi-photon Laser Scanning Microscope FV1000 MPE using an Olympus XLPLN 25X WMP water-dipping objective.

For spectral analysis (lambda scans) of live trichomes, brief excitation at 720 nm with 12% laser power and 800 HV on the photomultiplier tube detector was used. To minimize damage to the storage cavity, 4 μsec $pixel^{-1}$ dwell time and 256 × 256 pixel density was applied and cavities that burst were excluded. Emission was collected from 400 to 600 nm with a 10 nm bandwidth. Storage cavity fluorescence was captured by tracing a region of interest (ROI) on the intensity projection (n = 12 cavities per trichome type). ROI emission was plotted using Olympus FV10- ASW v3.01.

All subsequent 2P imaging was acquired with 720 nm excitation, and emission was captured using a BFP/GFP/RFP/DsRed filter cube in two channels, RXD1 (420–460 nm, false-coloured teal) and RXD2 (495–540 nm, false-coloured red). Images were processed and analyzed using ImageJ/FIJI (Schneider *et al.*, 2012). Images are presented as maximum intensity Z-projections.

Largest droplet diameter measurements were performed by scanning through the Z-stack of images containing the extracellular cavity of each trichome, identifying the largest droplet and measuring the greatest edge-to-edge length within the droplet. For cavity fluorescence ratio measurements, maximum intensity Z-projections of images containing only cavity fluorescence were produced and measured using FIJI. Fluorescence emission from the trichome cavity was quantified by comparing emission intensity in the cavity to a ROI containing no plant tissue within the same image. Corrected total cavity fluorescence (CTCF) of each emission channel was determined by the following equation: CTCF = Area Integrated Density of cavity − (Area of cavity × mean pixel fluorescence of background ROI). Cavity fluorescence ratio was determined by dividing the CTCF of the teal channel by the CTCF of the red channel.

Statistical analysis of the fluorescence and droplet diameter measurements were performed using the Statistical Package for the Social Sciences (SPSS v.25.0). A Kruskal–Wallis test revealed that distributions of both fluorescence ratio measurements and droplet diameters were not similar for all trichome groups, as assessed by visual inspection of the boxplots (Figure S1).

Disc cell counting

From three plants of the 'Finola' and 'Purple Kush' varieties of cannabis, at least three biological replicates of vegetative leaves (1 mm^2 dissections) and whole calyces (3–6 mm) were dissected and chemically fixed in 4% paraformaldehyde in PME buffer (25 mM PIPES, 5 mM $MgSO_4$, 5 mM EGTA) overnight at 4°C. After three washes in Tris-buffered saline/Tween (TBST), the tissues were transferred to a mixture of chloral hydrate/glycerol/water (8:1:2) and incubated for at least 3 days at room temperature on a rotary shaker. Length of clearing required was dependent on size of tissue, and each sample was observed daily until the epidermis

was translucent. The tissues were transferred to 0.2–1 μg ml^{-1} DAPI (Sigma, Oakville, Canada) in distilled water, wrapped in tinfoil, and incubated at room temperature for at least 10 min. Samples were rinsed for 24 h in distilled water at room temperature, followed by sample preparation and image acquisition as described in the live-cell 2-P section above. Images were analyzed using FIJI, where cells were counted using identifiable nuclei. Statistical analysis was performed using SPSS v.25.0.

Cryo-SEM analysis

After bract removal, dissected female cannabis flowers were attached to a universal freeze fracture specimen holder (Leica Microsystems, Concord, ON, Canada) with Tissue-Tek (VWR 25608-930, Mississauga, ON, Canada) and frozen under high vacuum in a cryo preparation unit (Emitech K1250, Quorum Technologies, Puslinch, ON, Canada) Using the Leica EM VCT100 cryo transfer system, samples were shuttled from the preparation unit to a cryo-scanning electron microscope (Hitachi S-4700 Field Emission, Krefeld, Germany), pre-cooled to −140°C. Sublimation at −105°C for 20 min was applied to remove surface ice. Images were captured with 1.0 kV and 15–20 mm working distance. In total, nine flowers were examined, prepared in three independent experiments.

Sample preparation for stitched SEM

Individual cannabis flowers were fixed in 0.025 M PIPES buffer with 2% v/v glutaraldehyde at pH 7.0 overnight at 4°C. Samples were rinsed in buffer twice then dehydrated with an ascending grade ethanol series of 30, 50, 70, 95, and 100% for 20 min each, with two additional 100% ethanol exchanges. This was followed by critical-point drying with solvent-substituted liquid CO_2 (Autosamdri 815B, Tousimis, Rockville, MD, USA), and sample mounting on aluminum specimen stubs. Samples were rotary coated with 5–12 nm of platinum (Cressington 208C high resolution sputter coater) and imaged in variable pressure mode with a Zeiss EVO or Sigma SEM at 10 kV and 2.5 nA at a working distance between 20 and 30 mm. Mosaic secondary electron (SE) images of entire calyces were collected at 500 nm per pixel and stitched using Zeiss Atlas 5 software.

Transmission electron microscopy

Samples were fixed and dehydrated as described for conventional SEM. After ethanol dehydration, samples were embedded with an ascending grade Spurr's resin series of 10, 20, 40, 60, 80, 95 and 100% for at least 3 h each. Two additional 100% resin exchanges were performed over 24 h, then samples were embedded in fresh 100% Spurr's resin in Beem capsules (Ted Pella, Redding, CA, USA) and polymerized at 60°C for 48 h. Here, 70 nm gold sections were cut using a Leica Ultramicrotome UCT, mounted on copper grids coated with 0.3% formvar, and post-stained with 2% uranyl acetate and lead citrate for 20 and 10 min, respectively. Imaging of sections was performed using a Hitachi 7600 transmission electron microscope operating at 80 kV.

UV-light assisted microextraction

Using microcapillaries (Microcaps; Drummond, Broomall, PA, USA) pulled to a fine point with a micropipette puller (Inject-Matic, Geneva, Switzerland) and a micromanipulator (MK1; Singer Instruments, Somerset, UK), metabolites were extracted specifically from 100 male antherial sessile, 200 female foliar sessile or 100 female floral stalked glandular trichomes. Glandular trichome identification was aided by a stereomicroscope (SZX10; Olympus, Toronto, Canada) equipped with a UV-light attachment (NIGHTSEA Stereo Microscope Fluorescence Adapter, Electron Microscopy Sciences). Extracts were collected by breaking resin-filled microcapillaries directly into GC vials (Supelco headspace vials with polytetrafluoroethylene (PTFE) silicone caps, Sigma, Oakville, Canada kept on dry ice during dissections, then stored at −80°C.

Solid-phase microextraction (SPME) GC-MS

Following UV-light assisted microextraction of trichome metabolites, terpene content was analyzed by the solid-phase microextraction technique on an Agilent 7890A/5975C Inert XL MSD Triple Axis gas chromatograph mass spectrometer equipped with an Agilent GC Sampler 80 autosampler. Supelco SPME 50/30 μm DVB/CAR/PDMS fiber and Agilent DB-WAX Column (30 m, 0.25 mm internal diameter, 0.25 μm film thickness) were used. The SPME GC-MS cycle included a 300 sec pre-incubation, 40°C incubation on SPME GC agitator unit, 600 sec extraction (fiber exposure), and 300 sec desorption, with an oven program of 35°C for 4 min, then increase 4° per min to 110°C, then increase 3° per min to 150°C, then increase 25° per min to 230°C and hold for 3 min. The helium flow rate was 0.9 ml min^{-1} and injection was split with a ratio of 4:1. The MS acquisition was performed in electron ionization mode with a mass range from 33.0 to 400.0. Selected ion monitoring was performed simultaneously for masses 93, 121, 136, 161, 189 and 204 with a dwell of 35. Data processing was performed with the Enhanced Chem Station and mass spectra were matched against NIST/WILEY library spectra (W9N08).

Microcapillary-sampled trichome cannabinoid analysis via ultraperformance liquid chromatography tandem mass spectrometry (UPLC)-MS/MS

Following SPME GC-MS, 50 μl of solvent (80 ACN:20 H_2O) was added to each GC vial and vortexed vigorously to dissolve metabolites associated with microcapillary fragments. The solution was separated from glass fragments by careful pipetting and placed in a high recovery silanized glass autosampler vial (Canadian Life Sciences). The UPLC-MS/MS apparatus (Waters Acquity H-Class with Xevo TQD) was equipped with an APCI probe in positive detection mode and a BEH C8 column (length 2.1 × 100 mm, i.d. 1.7 μm). Sample separation was performed with a mobile phase A: 0.1% formic acid (FA) in liquid chromatography mass spectrometry (LC-MS) grade H_2O and mobile phase B: 0.1% FA in LCMS grade acetonitrile, a flow rate of 0.6 ml min^{-1}, and injection volume of 5 μl, autosampled at 15°C. The program was as follows: 0 min: 48% B; 0–5 min: 48–83% B; 5–5.01 min: 83–95.2% B; 5.01–6 min 95.2% B; 6–6.01 min 95.2–47.7% B. A cannabinoid standards mixture (see Table S5, Cayman Chemical Company, Ann Arbor, MI, USA) at concentrations ranging from 100 to 100 000 ng ml^{-1} was used to generate a calibration curve, and the mixture at concentrations of 1000, 5000 and 25 000 ng ml^{-1} was run between sample sets for quality control. Data processing was performed with MassLynx v4.1 and comparison with standards' retention times and mass spectra.

Trichome type-specific enrichment by filtration and density gradient centrifugation

Using previously developed trichome isolation procedures (Gershenzon *et al.*, 1992; Sallets *et al.*, 2014) as a guide, 18–20 g of cannabis floral clusters (bud) was freshly removed from a female plant. The majority of flowers on each selected plant had calyces between the immature (<4 mm length with no observable stalked trichomes) and mature (>4 mm length with >70% stalked

trichomes) stages of development. This developmental range was selected to capture sessile, stalked and bulbous trichomes simultaneously and within the secretory phase of metabolite production. Trichomes were exposed by excising buds with scissors. Plant tissues were placed in a pre-chilled BeadBeater (BioSpec 1107900, Bartlesville, OK, USA) with Amberlite XAD4 (1 g g^{-1} plant material; Sigma) and 4°C isolation buffer (0.6% w/v methyl cellulose, 1% w/v PVP[3] MW 40000, 25 mM HEPES, 200 mM sorbitol, 10 mM sucrose, 10 mM KCl, 5 mM $MgCl_2$-$6H_20$, 0.5 mM KH_2PO_4) to full volume. The sealed chamber was submerged in ice for 30 min. All subsequent steps were performed at 4°C. Plant materials were blended with three short pulses separated by 30 sec cooling intervals and filtered through a 250-μm nylon mesh. The filtration residue was rinsed with cold wash buffer (consisting of all isolation buffer components, except methyl cellulose and PVP[3]) to obtain 1 L of filtrate. Second and third filtration steps were performed with pre-wetted 102 and 54 μm mesh nylon mesh, respectively, leaving sessile and stalked trichome heads on the filter surface. Trichomes were gently collected in round-bottom tubes (Fisher Scientific 14-959-10B, Ottawa, ON, Canada) with a 10 ml transfer pipette and wash buffer. To obtain bulbous trichomes from the filtrate, three additional filtrations through 54 μm nylon mesh were performed, followed by a final filtration through 25 μm mesh (Bubble Bag OGS1). The bulbous trichome fraction was obtained from the final filter surface.

All culture tubes containing trichome fractions were balanced by weight and pelleted in a swing bucket centrifuge (Eppendorf 5810R; 420 rpm, 4 min at 4°C). The pellets were gently resuspended in 6 ml (for sessile and stalked-enriched fractions) or 2 ml (for bulbous-enriched fractions) of wash buffer. To separate sessile and stalked trichome heads (consisting of a secretory disc with intact storage cavity), trichomes were layered onto a 100/35/15 density gradient consisting of 3 ml of 100% Percoll (Sigma-Aldrich P1644), 4 ml of 35%, and 4 ml of 15% Percoll in wash buffer. Multiple density gradients with trichomes were prepared, balanced and spun at 300 rpm for 15 min, 4°C. After centrifugation, a sessile-enriched upper band and stalked-enriched lower band was visible. Each band was collected in separate round-bottom tubes, resuspended in 14 ml wash buffer, pelleted (420 rpm, 4 min, 4°C) and gently resuspended in 5 ml of wash buffer to remove Percoll.

To harvest enriched trichome fractions, 0.5 ml aliquots of each trichome type were collected in 2 ml microcentrifuge tubes, leaving 1 ml for trichome type scoring. Each tube was diluted with 1 ml wash buffer, spun at full speed in a chilled microcentrifuge, the supernatant removed and the pellet was frozen in liquid nitrogen. All pellets were stored at −80°C.

To assess trichome type separation efficacy, samples from each gradient fraction were placed on a slide beneath a coverslip (22 × 40 mm) for visual scoring with a Leica DMR microscope. The presence of each trichome type with an intact storage cavity was recorded, along with the number of trichome discs (lacking intact cavities). Scoring was performed for a single pass along the length of a coverslip using a ×20 objective and UV filter to aid trichome type identification. Under brightfield and UV light, sessile trichome heads appeared granular and fluoresced green, respectively. In contrast, stalked trichome heads appeared homogenous and fluoresced blue.

RNA extraction, sequencing and transcriptome analysis

Using trichomes separated by type, RNA extractions were performed with a RNeasy Plant Mini Kit (Qiagen, Germantown, MD, USA), including the DNase digestion. Each RNA sample was further cleaned by ethanol precipitation by adding DNase/RNase-free H_2O to a total volume of 500 μl, 50 μl of sodium acetate (3 M, pH 5.2) and 1 ml ice cold 100% ethanol. Following 1 h incubation at −20°C, RNA was pelleted (4°C, 18 000 ***g***, 30 min) and rinsed with ice cold 70% ethanol and pelleted (4°C, 18 000 ***g***, 15 min). Each dried RNA pellet was resuspended in 30 μl RNase-free H_2O. RNA quality was assessed on a 0.8% agarose gel and NanoDrop spectrophotometer. For gel analysis, each sample was combined with formamide (see Masek *et al.*, 2005) and denatured at 65°C, 5 min prior to loading. RNA with a NanoDrop $OD_{260/280}$ of 1.8–2 and $OD_{260/230}$ of 1.8 or greater were deemed acceptable.

Sequencing libraries were prepared from 500 ng of total RNA using the TruSeq Stranded mRNA Sample Preparation kit (Illumina, San Diego, CA, USA) by the Sequencing and Bioinformatics Consortium (Dept. of Pharmaceutical Sciences, UBC Vancouver). Libraries were multiplexed and sequenced on a HiSeq 2500 in rapid run mode, generating paired-end 100 bp reads. Raw FASTQ reads were trimmed and quality filtered with trimmomatic v0.35m (Bolger *et al.*, 2014) using default settings except the following; LEADING:20, TRAILING:20, SLIDINGWINDOW:4:20, AVGQUAL:20, and MINLEN:40. Alignment of filtered reads against the *Cannabis sativa* reference transcriptomes, namely canSat3 and finola1 (van Bakel *et al.*, 2011), were performed using the bowtie2 v2.3.0 program using default settings (Langmead and Salzberg, 2012). Read summarization was performed with htseq-count v0.7.0 software (Anders *et al.*, 2015) with default parameters using the reference transcriptome annotation of canSat3 and finola1. Differential expression analysis was performed using the DESeq2 program (Love *et al.*, 2014). An FDR <0.05 defines differentially expressed transcripts between the tissue contrasts. Transcript abundance were expressed as fragments per kilobase of transcript per million mapped reads (FPKM) using DESeq2 and the length of predicted PK and FN transcripts. Enrichment of MapMan BIN categories (Thimm *et al.*, 2004) of differentially expressed genes were evaluated for enrichment using Fisher's exact test adjusted with FDR for multiple hypothesis correction according to previously established workflows (Wong *et al.*, 2017) using MapMan BIN-annotated PK and FN transcriptomes. MapMan BIN categories were considered significantly enriched in respective comparisons at a FDR < 0.05.

To enable robust comparisons between our trichome-enriched transcriptomes and the ones obtained from van Bakel *et al.* (2011) (i.e. root, shoot, stem, and flowers), the same RNA-seq processing workflow was performed and summarized as a whole. RNA-seq gene co-expression networks were constructed using log_2-transformed FPKM values using the Pearson's correlation coefficient as the metric of similarity. A 'guide' gene co-expression analysis was performed on selected candidate(s) and their top 300 co-expressed genes (ranked by descending PCC value) were analyzed further.

Atlas analysis

Image analysis was performed using the Atlas browser export software. The length of each calyx was measured using the point-to-point measurement tool along the medial axis of the calyx from base to tip. Glandular trichomes were counted within 500–1000 μm^2 areas of the mid-section of each calyx, with each area containing a minimum of 25 trichomes. Trichomes were annotated as a stalked glandular trichome if the presence of a stalk could be seen at high magnification. Sessile glandular trichomes were annotated based on the absence of a stalk, and a minimum gland diameter of 25 μm.

TPS cloning and characterization

Total RNA was isolated from 'Finola' flowers using the Invitrogen PureLink Plant RNA reagent (www.thermofisher.com). RNA quality and concentration was measured using the Bioanalyzer 2100 RNA Nanochip assay (www.agilent.ca). Full-length sequences of FN15171.1 and FN20433.1 were obtained using 5′ Rapid Amplification of cDNA ends (5′-RACE) (www.clontech.com). 5′ Plastid target peptides were predicted using the TargetP algorithm (Emanuelsson *et al.*, 2000). Sequences were truncated to the RRX_8W motif (Bohlmann *et al.*, 1998) and cloned into the pASK IBA37 vector (www.iba-lifesciences.org) with a 5′ 6X-HIS tag.

Vectors were transformed into *E. coli* strain BL21DE3 for heterologous protein expression. Bacterialcultures were grown in 50 ml Luria Broth containing ampicillin (100 mg ml^{-1}). Cultures were grown at 37°C at 200 rpm until they reached OD_{600} 0.6, then at 18°C for another 2 h. Protein production was then induced using 200 μg L^{-1} anhydrous tetracycline, and the cultures were shaken for a further 18 h before harvesting by centrifugation.

Recombinant protein was purified using the GE Healthcare His SpinTrap kit (www.gelifesciences.com) according to the manufacturer's instructions. Binding buffer for purification was 20 mM 2-[4-(2-hydroxyethyl)piperazin-1-yl]ethanesulfonic acid (HEPES) (pH 7.5), 500 mM NaCl, 25 mM imidazole, and 5% glycerol. Cells were lysed in binding buffer supplemented with Roche complete protease inhibitor tablets (lifescience.roche.com) and 0.1 mg ml^{-1} lysozyme. Elution buffer was 20 mM HEPES (pH 7.5), 500 mM NaCl, 350 mM imidazole, and 5% glycerol. Purified protein was desalted through Sephadex into TPS assay buffer.

In vitro assays were performed at 500 μl volume by incubating purified protein with isoprenoid diphosphate substrates as previously described (O'Maille *et al.*, 2004). TPS assay buffer was 25 mM HEPES (pH 7.5), 100 mM KCl, 10 mM MgCl2, 5% glycerol, and 5 mM DTT. GPP was dissolved in 50% methanol and used at 32 μM. Assays were overlaid with 500 μl pentane containing 31 g L^{-1} isobutyl benzene as internal standard.

Product identification was performed using an Agilent 7890A gas chromatographer with a 7683B series autosampler and a 7000A TripleQuad mass spectrometer. Ionization was at 70 eV electrospray with a flow rate of 1 ml min^{-1} of He. The column was an Agilent VP-5MS (30 m, 250 μm internal diameter, 0.25 μm film). The temperature program was: 50°C for 1 min, then increased at 10°C per min to 280°C, then held for 5 min. Injection was 1 μl pulsed splitless. Products were identified by comparison with authentic standards.

Whole-organ metabolite analysis

Metabolite analysis was performed on whole organs from 5 'Finola' plants harvested at week 7 post-seed germination (immature calyces) and week 13 post-seed germination (mature calyces and mature vegetative leaves). Three floral clusters were harvested for each time point, one from an axillary bud of a lateral branch from the first node (oldest flowers), one from an axillary bud near the shoot apex, and one from the tip of the main cola (youngest flowers). Three replicate calyces were dissected from each cluster and used for metabolite analysis. At least three vegetative leaves were harvested from the shoot base at the oldest branching nodes. Calyces were immature if there were no conspicuous stalked trichomes and the calyx was less than 4 mm in length, while mature calyces contained >70% stalked trichomes and greater than 4 mm in length, as assessed on an Olympus SZX10 stereomicroscope. Vegetative leaves were devoid of stalked glandular trichomes.

Whole calyces were immersed in 500 μl of pentane with 31 g L^{-1} isobutyl benzene as internal standard. Resin was extracted by vigorous vortexing with glass beads followed by shaking for 4 h at room temperature. Tissue was dried at 60°C for 16 h, then weighed. The same procedure was followed for leaves, but using 4 ml of solvent.

Compounds were identified using the same GC-MS equipment as above, but with the following temperature program: 50°C for 3 min, then increased at 10°C per min to 150°C, then increased at 15°C per min to 320°C, and held for 5 min. Identifications were made by comparison with authentic standards and NIST/WILEY library spectra. Monoterpenes were quantified using standard curves of α-pinene, myrcene, limonene and linalool. Sesquiterpenes were quantified using β-caryophyllene, (*E*)-β-farnesene, and bisabolol standard curves. No standards were available for cannabinoids, so THC and CBD were identified by retention index and quantified by relative peak area.

Whole-organ cannabinoid analysis via UPLC-MS/MS

Following GC-MS, 10 μl of pentane extract was evaporated to dryness under a thin stream of nitrogen and resuspended in 1 ml acetonitrile (CAN). The UPLC-MS/MS apparatus (Waters Acquity H-Class with QDa) was run in electrospray ionization (ESI) detection mode and a Raptor ARC-C18 column (length 2.1 × 150 mm, i.d. 2.7 μm). Sample separation was performed with a mobile phase A: 0.1% FA in LCMS grade H_2O and mobile phase B: 0.1% FA in LCMS grade ACN, a flow rate of 0.6 ml min^{-1}, and injection volume 5 μl, autosampled at 15°C. The program was as follows: 0 min: 72% B; 1–3 min: 72–84.5% B; 3–3.6 min: 84.6–100% B; 3.8–5 min 100–72% B. A cannabinoid standards mixture (Cerilliant, see Table S6) at concentrations ranging from 40 to 20 000 ng ml^{-1} was used to generate a calibration curve, and the mixture at concentrations of 1000, 5000 and 25 000 ng ml^{-1} was run between sample sets for quality control. Standards (Syst. Suit inje. 1–5 at 320 ng ml^{-1}) were analyzed. Data processing was performed with MassLynx v4.1 and comparison with standards' retention times and mass spectra.

ACCESSION NUMBERS

All raw sequencing data were deposited in the NCBI Sequence Read Archive (http://www.ncbi.nlm.nih.gov/sra) under the BioProject and SRA accession of PRJNA483805 and SRP155904, respectively. Sequences for TPS37 and TPS38 were deposited into NCBI GenBank (https://www.ncbi.nlm.nih.gov/genbank/) with the accession numbers MK614216 and MK614217 respectively.

ACKNOWLEDGEMENTS

Funding for this project came from the Canadian Natural Sciences and Engineering Research Council Discovery Grants to ALS, SDC, and JB; and a Mitacs Elevate Post-doctoral Fellowship, in partnership with Anandia Laboratories, to TDQ. The authors thank Lina Madilao for GC method development, John Coleman for UPLC, Sunita Sinha at the Sequencing and Bioinformatics Consortium (Department of Pharmaceutical Sciences, UBC Vancouver) and Leo Law and Shisen Wang for technical assistance. The authors would like to thank the many Anandia employees involved in plant cultivation and maintenance throughout the duration of the project. The authors thank Elizabeth Samuels, Dr. Raju Datla, and Tonya Severson for constructive comments on the manuscript. The laboratory of Professor Nelly Panté kindly provided the

equipment for microcapillary sampling. The technical assistance of the UBC Bioimaging Facility is gratefully acknowledged.

CONFLICT OF INTEREST

Jonathan Page is the CSO of Aurora Cannabis Inc., a cannabis license producer and biotechnology company. Kim Rensing is an employee at Fibics, Inc., the software company producing the Atlas software used in this study.

AUTHOR CONTRIBUTIONS

SJL, TDQ, JEP and ALS conceived and designed the experiments. Cryo-SEM imaging was performed by TDQ. TEM was performed by SJL. 2P live-cell imaging and analysis was performed by SJL and TDQ. DAPI imaging and analysis was performed by SJL and JLY. Conventional SEM was imaged by SJL, TDQ, and KHR and analyzed by SJL. Microcapillary sampling was performed and analyzed by TDQ. Whole-organ dipping was performed and analyzed by JKB. *In vitro* TPS-b characterization was performed by JKB. Trichome isolation and enrichment for RNA-seq was prepared by TDQ and transcriptome analysis by DCJW. SJL, TDQ and ALS wrote the manuscript with major input from JKB, KHR, DCJW, SDC, JB and JEP.

SUPPORTING INFORMATION

Additional Supporting Information may be found in the online version of this article.

Figure S1. Two-photon imaging and disc cell counting of high-THCA medicinal cannabis varieties 'Purple Kush' and 'Hindu Kush'.

Figure S2. Statistical analyses (distributions and pair-wise comparisons) of droplet size and fluorescence ratio measurements.

Figure S3. Terpene profiles and chromatograms from whole-organ solvent extractions.

Figure S4. Terpene profiles and chromatograms from microcapillary-extracted trichome sampling.

Figure S5. Summary of highly expressed genes according to their functional categories in cannabis glandular trichomes.

Figure S6. Summary of enriched MAPMAN functional categories of differentially expressed cannabis glandular trichome genes.

Figure S7. Maximum likelihood phylogeny of terpene synthase amino acid sequences.

Table S1. Summary of RNA-seq analysis metrics.

Table S2. Differentially expressed genes whose expression was higher in stalked or sessile trichomes compared with bulbous trichomes.

Table S3. Highly expressed cannabinoid biosynthetic genes in cannabis trichomes.

Table S4. Terpene synthase gene expression and characterization in isolated glandular trichomes.

Table S5. Xevo TQD conditions for the analysis of 10 cannabinoids.

Table S6. QDa conditions for the analysis of 10 cannabinoids.

Data S1. Complete list of transcripts in stalked, pre-stalked and bulbous trichomes.

Data S2. Detailed list of enriched MAPMAN functional categories of stalked versus bulbous and pre-stalked versus bulbous.

Data S3. Complete list of transcripts in stalked and pre-stalked trichomes that are differentially expressed compared to bulbous trichomes.

Data S4. Top 300 most highly co-expressed genes with CBDAS.

Video S1. Example of ATLAS multi-scale SEM imaging of cannabis calyx.

REFERENCES

Aizpurua-Olaizola, O., Soydaner, U., Öztürk, E., Schibano, D., Simsir, Y., Navarro, P., Etxebarria, N. and Usobiaga, A. (2016) Evolution of the cannabinoid and terpene content during the growth of *Cannabis sativa* plants from different chemotypes. *J. Nat. Prod.* **79**, 324–331.

Anders, S., Pyl, P.T. and Huber, W. (2015) HTSeq—a Python framework to work with high-throughput sequencing data. *Bioinformatics*, **31**, 166–169.

van Bakel, H., Stout, J.M., Cote, A.G., Tallon, C.M., Sharpe, A.G., Hughes, T.R. and Page, J.E. (2011) The draft genome and transcriptome of *Cannabis sativa*. *Genome Biol.* **12**, R102.

Balcke, G.U., Bennewitz, S., Bergau, N., Athmer, B., Henning, A., Majovsky, P., Jiménez-Gómez, J.M., Hoehenwarter, W. and Tissier, A. (2017) Multiomics of tomato glandular trichomes reveals distinct features of central carbon metabolism supporting high productivity of specialized metabolites. *Plant Cell*, **29**, 960–983.

Bergau, N., Bennewitz, S., Syrowatka, F., Hause, G. and Tissier, A. (2015) The development of type VI glandular trichomes in the cultivated tomato *Solanum lycopersicum* and a related wild species *S. habrochaites*. *BMC Plant Biol.* **15**, 289–304.

Bergau, N., Santos, A.N., Henning, A., Balcke, G.U. and Tissier, A. (2016) Autofluorescence as a signal to sort developing glandular trichomes by flow cytometry. *Front. Plant Sci.* **7**, 949.

Bohlmann, J., Meyer-Gauen, G. and Croteau, R. (1998) Plant terpenoid synthases: molecular biology and phylogenetic analysis. *Proc. Natl Acad. Sci. USA*, **95**, 4126–4133.

Bolger, A.M., Lohse, M. and Usadel, B. (2014) Trimmomatic: a flexible trimmer for Illumina sequence data. *Bioinformatics*, **30**, 2114–2120.

Booth, J.K. and Bohlmann, J. (2019) Terpenes in *Cannabis sativa*- from plant genome to humans. *Plant Sci.* **284**, 67–72

Booth, J.K., Page, J.E. and Bohlmann, J. (2017) Terpene synthases from *Cannabis sativa*. *PLoS One*, **12**, e0173911.

Celedon, J.M., Chiang, A., Yuen, M.M.S., Diaz-Chavez, M.L., Madilao, L.L., Finnegan, P.M., Barbour, E.L. and Bohlmann, J. (2016) Heartwood specific transcriptome and metabolite signatures of tropical sandalwood (*Santalum album*) reveal the final step of (*Z*)-santalol fragrance biosynthesis. *Plant J.* **86**, 289–299. https://doi.org/10.1111/tpj.13162.

Dayanandan, P. and Kaufman, P.B. (1976) Trichomes of *Cannabis sativa* (Cannabaceae). *Am. J. Bot.* **63**, 578–591.

Ebersbach, P., Stehle, F., Kayser, O. and Freier, E. (2018) Chemical fingerprinting of single glandular trichomes of *Cannabis sativa* by coherent anti-Stokes raman scattering (CARS) microscopy. *BMC Plant Biol.* **18**, 275.

Emanuelsson, O., Nielsen, H., Brunak, S. and von Heijne, G. (2000) Predicting subcellular localization of proteins based on their N-terminal amino acid sequence. *J. Mol. Biol.* **300**, 1005–1016.

Fischedick, J.T., Hazekamp, A., Erkelens, T., Choi, Y.H. and Verpoorte, R. (2010) Metabolic fingerprinting of *Cannabis sativa* L., cannabinoids and terpenoids for chemotaxonomic and drug standardization purposes. *Phytochemistry*, **71**, 2058–2073.

Gagné, S.J., Stout, J.M., Liu, E., Boubakir, Z., Clark, S.M. and Page, J.E. (2012) Identification of olivetolic acid cyclase from *Cannabis sativa* reveals a unique catalytic route to plant polyketides. *Proc. Natl Acad. Sci. USA*, **109**, 12811–12816.

Gershenzon, J., McCaskill, D., Rajaonarivony, J.I.M., Mihaliak, C., Karp, F. and Croteau, R. (1992) Isolation of secretory cells from plant glandular trichomes and their use in biosynthetic studies of monoterpenes and other gland products. *Anal. Biochem.* **200**, 130–138.

Glas, J.J., Bernardus, C.J.S., Alba, J.M., Escobar-Bravo, R., Schuurink, R.C. and Kant, M.R. (2012) Plant glandular trichomes as targets for breeding or engineering of resistance to herbivores. *Int. J. Mol. Sci.* **13**, 17077–17103.

Hammond, C.T. and Mahlberg, P.G. (1973) Morphology of glandular hairs of *Cannabis sativa* from scanning electron microscopy. *Am. J. Bot.* **60**, 524–528.

Hammond, C.T. and Mahlberg, P.G. (1977) Morphogenesis of capitate glandular hairs of *Cannabis sativa* (*Cannabaceae*). *Am. J. Bot.* **64**, 1023.

Happyana, N., Agnolet, S., Muntendam, R., Van Dam, A., Schneider, B. and Kayser, O. (2013) Analysis of cannabinoids in laser-microdissected trichomes of medicinal Cannabis sativa using LCMS and cryogenic NMR. *Phytochemistry*, **87**, 51–59.

Hazekamp, A., Peltenburg, A., Verpoorte, R. and Giroud, C. (2005) Chromatographic and spectroscopic data of cannabinoids from *Cannabis sativa* L. *J. Liq. Chromatogr. Relat. Technol.* **28**, 2361–2382.

Hillig, K.W. (2004) A chemotaxonomic analysis of terpenoid variation in Cannabis. *Biochem. Syst. Ecol.* **32**, 875–891.

Huang, S.-S., Kirchoff, B.K. and Liao, J.-P. (2008) The capitate and peltate glandular trichomes of *Lavandula pinnata* L. (Lamiaceae): histochemistry, ultrastructure and secretion. *J. Torrey Bot. Soc.* **135**, 155–167.

Huchelmann, A., Boutry, M. and Hachez, C. (2017) Plant glandular trichomes: natural cell factories of high biotechnological interest. *Plant Physiol.* **175**, 6–22.

Hwang, J.U., Song, W.Y., Hong, D. *et al.* (2016) Plant ABC transporters enable many unique aspects of a terrestrial plant's lifestyle. *Mol. Plant*, **9**, 338–355.

Johnson, S.R., Lange, I., Narayanan, S. and Lange, B.M. (2017) Bioenergetics of monoterpenoid essential oil biosynthesis in nonphotosynthetic glandular trichomes. *Plant Physiol.* **175**, 681–695.

Kim, E.S. and Mahlberg, P.G. (1991) Secretory cavity development in glandular trichomes of Cannabis sativa L. *Am. J. Bot.* **78**, 220–229.

Kim, E.S. and Mahlberg, P.G. (2003) Secretory vesicle formation in the secretory cavity of glandular trichomes of Cannabis sativa L. (Cannabaceae). *Mol. Cells*, **15**, 387–395.

Lange, B.M. (2015a) The evolution of plant secretory structures and emergence of terpenoid chemical diversity. *Annu. Rev. Plant Biol.* **66**, 139–159.

Lange, I., Poirier, B.C., Herron, B.K. and Lange, B.M. (2015b) Comprehensive assessment of transcriptional regulation facilitated metabolic engineering of isoprenoid accumulation in Arabidopsis. *Plant Physiol.* **169**, 1595–1606.

Langmead, B. and Salzberg, S.L. (2012) Fast gapped-read alignment with Bowtie 2. *Nat. Methods*, **9**, 357–359.

Liu, C., Srividya, N., Parrish, A.N., Yue, W., Shan, M., Wu, Q. and Lange, B.M. (2018) Morphology of glandular trichomes of Japanese catnip (*Schizonepeta tenuifolia* Briquet) and developmental dynamics of their secretory activity. *Phytochemistry*, **150**, 23–30.

Love, M.I., Huber, W. and Anders, S. (2014) Moderated estimation of fold change and dispersion for RNA-seq data with DESeq2. *Genome Biol.* **15**, 550.

Mahlberg, P.G. and Kim, E.S. (2004) Accumulation of cannabinoid in glandular trichomes of *Cannabis* (*Cannabaceae*). *J. Ind. Hemp*, **9**, 15–36.

Malingré, T., Hendriks, H., Batterman, S., Bos, R. and Visser, J. (1975) The essential oil of Cannabis sativa. *Planta Med.* **28**, 56–61.

Masek, T., Vopalensky, V., Suchomelova, P. and Pospisek, M. (2005) Denaturing RNA electrophoresis in TAE agarose gels. *Anal. Biochem.* **336**, 46–50.

McDowell, E.T., Kapteyn, J., Schmidt, A. *et al.* (2011) Comparative functional genomic analysis of *Solanum* glandular trichome types. *Plant Physiol.* **155**, 524–539.

Mechoulam, R. (1970) Marihuana chemistry. *Science*, **160**, 1467–1469.

Mediavilla, V. and Setinemann, S. (1997) Essential oil of *Cannabis sativa* L. strains. *J. Int. Hemp Assoc.* **4**, 80–82.

Meier, C. and Mediavilla, V. (1998) Factors influencing the yield and the quality of hemp (*Cannabis sativa* L.) essential oil. *J. Int. Hemp Assoc.* **5**, 16–20.

Mudge, E.M., Brown, P.N. and Murch, S.J. (2019) The Terroir of Cannabis: terpene metabolomics as a tool to understand Cannabis sativa selections. *Planta Med.* **85**, 781–796.

O'Maille, P.E., Chappell, J. and Noel, J.P. (2004) A single-vial analytical and quantitative gas chromatography-mass spectrometry assay for terpene synthases. *Anal. Biochem.* **335**, 210–217.

Pertwee, R.G. (2008) The diverse CB1 and CB2 receptor pharmacology of three plant cannabinoids: delta9-tetrahydrocannabinol, cannabidiol and delta9-tetrahydrocannabivarin. *Br. J. Pharmacol.* **153**, 199–215.

Pertwee, R.G. (ed). (2014) *Handbook of Cannabis*. Oxford, UK: Oxford University Press.

Potter, D.J. (2009). The propagation, characterisation and optimisation of cannabis as a phytopharmaceutical. Thesis, Kings College London. Available from: https://ia801604.us.archive.org/25/items/CANNABISSATIVAASAPHYTOPHARMACEUTICAL/THE%20PROPAGATION%2C%20CHARACTERISATION%20AND%20OPTIMISATION%20OF%20CANNABIS%20SATIVA%20AS%20A%20PHYTOPHARMACEUTICAL.pdf (Accessed October 25 2018).

Ross, S.A. and ElSohly, M.A. (1996) The volatile oil composition of fresh and air-dried buds of *Cannabis sativa*. *J. Nat. Prod.* **59**, 49–51.

Russo, E.B. (2011) Taming THC: potential cannabis synergy and phytocannabinoid-terpenoid entourage effects. *Br. J. Pharmacol.* **163**, 1344–1364.

Sallets, A., Beyaert, M., Boutry, M. and Champagne, A. (2014) Comparative proteomics of short and tall glandular trichomes of *Nicotiana tabacum* reveals differential metabolic activities. *J. Proteome Res.* **13**, 3386–3396.

Sawler, J., Stout, J.M., Garner, K.M., Hudson, D., Vidmar, J., Butler, L., Page, J.E. and Myles, S. (2015) The genetic structure of marijuana and hemp. *PLoS One*, **10**, e0133292.

Schilmiller, A.L., Last, R.L. and Pichersky, E. (2008) Harnessing plant trichome biochemistry for the production of useful compounds. *Plant J.* **54**, 702–711.

Schilmiller, A.L., Schauvinhold, I., Larson, M., Xu, R., Charbonneau, A.L., Schmidt, A., Wilkerson, C., Last, R.L. and Pichersky, E. (2009) Monoterpenes in the glandular trichomes of tomato are synthesized from a neryl diphosphate precursor rather than geranyl diphosphate. *Proc. Natl Acad. Sci. USA*, **106**, 10865–10870.

Schilmiller, A.L., Charbonneau, A.L. and Last, R.L. (2012) Identification of a BAHD acetyltransferase that produces protective acyl sugars in tomato trichomes. *Proc. Natl Acad. Sci. USA*, **109**, 16377–16382.

Schneider, C.A., Rasband, W.S. and Eliceiri, K.W. (2012) NIH Image to ImageJ: 25 years of Image Analysis. *Nat. Methods*, **9**, 671.

Schwender, J., König, C., Klapperstück, M. *et al.* (2014) Transcript abundance on its own cannot be used to infer fluxes in central metabolism. *Front. Plant Sci.* **5**, 668.

Simmons, A.T. and Gurr, G.M. (2005) Trichomes of *Lycopersicon* species and their hybrids: effects on pests and their natural enemies. *Agric. For. Entomol.* **7**, 265–276.

Small, E. and Naraine, S.G.U. (2016) Size matters: evolution of large drug-secreting resin glands in elite pharmaceutical strains of *Cannabis sativa* (marijuana). *Genet. Resour. Crop Evol.* **63**, 349–359.

Stout, J., Boubakir, Z., Ambrose, S.J., Purves, R.W. and Page, J.E. (2012) The hexanoyl-CoA precursor for cannabinoid biosynthesis is formed by an acyl-activating enzyme in Cannabis sativa trichomes. *Plant J.* **71**, 353–365.

Taura, F., Morimoto, S. and Shoyama, Y. (1996) Purification and characterization of cannabidiolic-acid synthase from *Cannabis sativa* L. Biochemical analysis of a novel enzyme that catalyzes the oxidocyclization of cannabigerolic acid to cannabidiolic acid. *J. Biol. Chem.* **271**, 17411–17416.

Taura, F., Tanaka, S., Taguchi, C., Fukamizu, T., Tanaka, H., Shoyama, Y. and Morimoto, S. (2009) Characterization of olivetol synthase, a polyketide synthase putatively involved in cannabinoid biosynthetic pathway. *FEBS Lett.* **583**, 2061–2066.

Thimm, O., Bläsing, O., Gibon, Y., Nagel, A., Meyer, S., Krüger, P., Silbig, J., Müller, L.A., Rhee, S.Y. and Stitt, M. (2004) MAPMAN: a user-driven tool to display genomics data sets onto diagrams of metabolic pathways and other biological processes. *Plant J.* **37**, 914–939.

Tissier, A. (2012) Glandular trichomes: what comes after expressed sequence tags? *Plant J.* **70**, 51–68.

Turner, J.C., Hemphill, J.K. and Mahlberg, P.G. (1977) Gland distribution and cannabinoid content in clones of *Cannabis sativa* L. *Am. J. Bot.* **64**, 687–693.

Turner, J.C., Hemphill, J.K. and Mahlberg, P.G. (1978) Quantitative determination of cannabinoids in individual glandular trichomes of *Cannabis sativa* L. (Cannabaceae). *Am. J. Bot.* **65**, 1103–1106.

Turner, G.W., Gershenzon, J. and Croteau, R. (2000) Development of peltate glandular trichomes of peppermint. *Plant Physiol.* **124**, 665–679.

Werker, E. (2000) Trichome diversity and development. *Adv. Bot. Res.* **31**, 1–35.

Wong, D.C.J., Gutierrez, R.L., Gambetta, G.A. and Castellarin, S.D. (2017) Genome-wide analysis of cis-regulatory element structure and discovery of motif-driven gene co-expression networks in grapevine. *DNA Res.* **24**, 311–326.

Xie, Z., Kapteyn, J. and Gang, D.R. (2008) A systems biology investigation of the MEP/terpenoid and shikimate/phenylpropanoid pathways points to multiple levels of metabolic control in sweet basil glandular trichomes. *Plant J.* **54**, 349–361.

Zager, J.J., Lange, I., Srividya, N., Smith, A. and Lange, B.M. (2019) Gene networks underlying cannabinoid and terpenoid accumulation in Cannabis. *Plant Physiol.* **180**, 1877–1897. https://doi.org/10.1104/pp.18.01506.